Density matrices and path integrals

3

In this chapter, we continue our parallel exploration of statistical and computational physics, but now move to the field of quantum mechanics, where the density matrix generalizes the classical Boltzmann distribution. The density matrix constructs the quantum statistical probabilities from their two origins: the quantum mechanical wave functions and the Boltzmann probabilities of the energy levels. The density matrix can thus be defined in terms of the complete solution of the quantum problem (wave functions, energies), but all this information is available only in simple examples, such as the free particle or the harmonic oscillator.

A simple general expression exists for the density matrix only at high temperature. However, a systematic convolution procedure allows us to compute the density matrix at any given temperature from a product of two density matrices at higher temperature. By iteration, we reach the density matrix at any temperature from the high-temperature limit. We shall use this procedure, matrix squaring, to compute the quantum-statistical probabilities for particles in an external potential.

The convolution procedure, and the connection it establishes between classical and quantum systems, is the basis of the Feynman path integral, which really opens up the field of finite-temperature quantum statistics to computation. We shall learn about path integrals in more and more complicated settings. As an example of interacting particles, we shall come back to the case of hard spheres, which model quantum gases and quantum liquids equally well. The path integral allows us to conceive of simulations in interacting quantum systems with great ease. This will be studied in the present chapter for the case of two hard spheres, before taking up the many-body problem in Chapter 4.

Classical particles are related to points, the pebbles of our first chapter. Analogously, quantum particles are related to one-dimensional objects, the aforementioned paths, which have important geometric properties. Path integrals, like other concepts of statistical mechanics, have spread to areas outside their field of origin, and even beyond physics. They are for example used to describe stock indices in financial mathematics. The final section of this chapter introduces the geometry of paths and related objects. This external look at our subject will foster our understanding of quantum physics and of the path integral. We shall reach analytical and algorithmic insights complementing those of earlier sections of the chapter.

Copyright © 2006. Oxford University Press, Incorporated. All rights reserved.

Krauth, Werner. Statistical Mechanics: Algorithms and Computations, Oxford University Press, Incorporated, 2006. ProQuest Ebook Central, http://ebookcentral.proquest.com/lib/tau/detail.action?docID=431021.
Created from tau on 2024-08-12 07:17:16.

A quantum particle in a harmonic potential is described by energies and wave functions that we know exactly (see Fig. 3.1). At zero temperature, the particle is in the ground state; it can be found with high probability only where the ground-state wave function differs markedly from zero. At finite temperatures, the particle is spread over more states, and over a wider range of x-values. In this chapter, we discuss exactly how this works for a particle in a harmonic potential and for more difficult systems. We also learn how to do quantum statistics if we ignore everything about energies and wave functions.

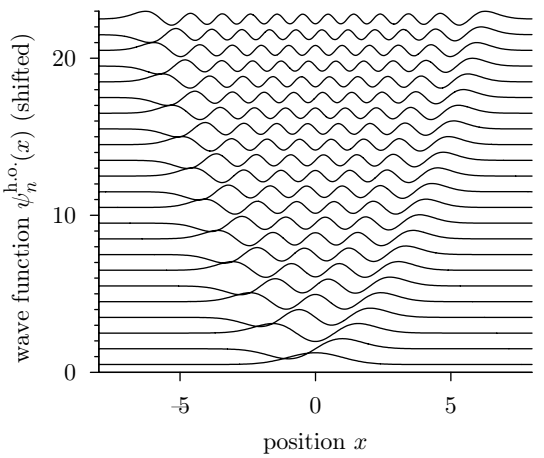

Fig. 3.1 Harmonic-oscillator wave functions $\psi_n^{\mathrm{h.o.}}(x)$ shifted by E_n (from Alg. 3.1 (`harmonic-wavefunction`)).

Copyright © 2006. Oxford University Press, Incorporated. All rights reserved.

Krauth, Werner. Statistical Mechanics: Algorithms and Computations, Oxford University Press, Incorporated, 2006. ProQuest Ebook Central, http://ebookcentral.proquest.com/lib/tau/detail.action?docID=431021.
Created from tau on 2024-08-12 07:17:16.

3.1 Density matrices

Quantum systems are described by wave functions and eigenvalues, solutions of the Schrödinger equation. We shall show for the one-dimensional harmonic oscillator how exactly the probabilities of quantum physics combine with the statistical weights in the Boltzmann distribution, before moving on to more general problems.

3.1.1 The quantum harmonic oscillator

The one-dimensional quantum mechanical harmonic oscillator, which consists of a particle of mass m in a potential

$$V(x) = \frac{1}{2} m\omega^2 x^2,$$

is governed by the Schrödinger equation

$$H\psi_n^{\text{h.o.}} = \left(-\frac{\hbar^2}{2m}\frac{\partial^2}{\partial x^2} + \frac{1}{2}m\omega^2 x^2 \right) \psi_n^{\text{h.o.}} = E_n \psi_n^{\text{h.o.}}. \tag{3.1}$$

procedure `harmonic-wavefunction`
input x
$\psi_{-1}^{\text{h.o.}}(x) \leftarrow 0$ (unphysical, starts recursion)
$\psi_0^{\text{h.o.}}(x) \leftarrow \pi^{-1/4} \exp\left(-x^2/2\right)$ (ground state)
for $n = 1, 2, \dots$ **do**
$\left\{ \quad \psi_n^{\text{h.o.}}(x) \leftarrow \sqrt{\frac{2}{n}} x \psi_{n-1}^{\text{h.o.}}(x) - \sqrt{\frac{n-1}{n}} \psi_{n-2}^{\text{h.o.}}(x) \right.$
output $\{\psi_0^{\text{h.o.}}(x), \psi_1^{\text{h.o.}}(x), \dots\}$

Algorithm 3.1 `harmonic-wavefunction`. Eigenfunctions of the one-dimensional harmonic oscillator (with $\hbar = m = \omega = 1$).

In general, the wave functions $\{\psi_0, \psi_1, \dots\}$ satisfy a completeness condition

$$\sum_{n=0}^{\infty} \psi_n^*(x)\psi_n(y) = \delta(x-y),$$

where $\delta(x-y)$ is the Dirac δ-function, and form an orthonormal set:

$$\int_{-\infty}^{\infty} \mathrm{d}x \; \psi_n^*(x)\psi_m(x) = \delta_{nm} = \begin{cases} 1 & \text{if } n = m \\ 0 & \text{otherwise} \end{cases}, \tag{3.2}$$

where δ_{nm} is the discrete Kronecker δ-function. The wave functions of the harmonic oscillator can be computed recursively[1] (see Alg. 3.1 (`harmonic-wavefunction`)). We can easily write down the first few of them, and verify that they are indeed normalized and mutually orthogonal, and that $\psi_n^{\text{h.o.}}$ satisfies the above Schrödinger equation (for $m = \hbar = \omega = 1$) with $E_n = n + \frac{1}{2}$.

[1] In most formulas in this chapter, we use units such that $\hbar = m = \omega = 1$.

Copyright © 2006. Oxford University Press, Incorporated. All rights reserved.

Krauth, Werner. Statistical Mechanics: Algorithms and Computations, Oxford University Press, Incorporated, 2006. ProQuest Ebook Central, http://ebookcentral.proquest.com/lib/tau/detail.action?docID=431021.
Created from tau on 2024-08-12 07:17:16.

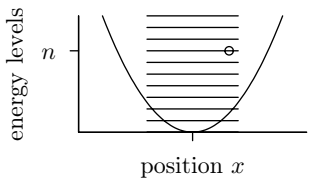

Fig. 3.2 A quantum particle at position x, in energy level n. The density matrix only retains information about positions.

In thermal equilibrium, a quantum particle occupies an energy state n with a Boltzmann probability proportional to $\mathrm{e}^{-\beta E_n}$, and the partition function is therefore

$$Z^{\text{h.o.}}(\beta) = \sum_{n=0}^{\infty} \mathrm{e}^{-\beta E_n} = \mathrm{e}^{-\beta/2} + \mathrm{e}^{-3\beta/2} + \mathrm{e}^{-5\beta/2} + \cdots$$
$$= \mathrm{e}^{-\beta/2}\left(\frac{1}{1-\mathrm{e}^{-\beta}}\right) = \frac{1}{\mathrm{e}^{\beta/2}-\mathrm{e}^{-\beta/2}} = \frac{1}{2\sinh(\beta/2)}. \quad (3.3)$$

The complete thermodynamics of the harmonic oscillator follows from eqn (3.3). The normalized probability of being in energy level n is

$$\left\{\begin{array}{c}\text{probability of being}\\ \text{in energy level } n\end{array}\right\} = \frac{1}{Z}\,\mathrm{e}^{-\beta E_n}.$$

When it is in energy level n (see Fig. 3.2), a quantum system is at a position x with probability $\psi_n^*(x)\psi_n(x)$. (The asterisk stands for the complex conjugate; for the real-valued wave functions used in most of this chapter, $\psi^* = \psi$.) The probability of being in level n at position x is

$$\left\{\begin{array}{c}\text{probability of being}\\ \text{in energy level } n\\ \text{at position } x\end{array}\right\} = \frac{1}{Z}\,\mathrm{e}^{-\beta E_n}\psi_n(x)\psi_n^*(x). \quad (3.4)$$

This expression generalizes the Boltzmann distribution to quantum physics. However, the energy levels and wave functions are generally unknown for complicated quantum systems, and eqn (3.4) is not useful for practical computations. To make progress, we discard the information about the energy levels and consider the (diagonal) density matrix

$$\pi(x) = \left\{\begin{array}{c}\text{probability of being}\\ \text{at position } x\end{array}\right\} \propto \rho(x,x,\beta) = \sum_n \mathrm{e}^{-\beta E_n}\psi_n(x)\psi_n^*(x),$$

as well as a more general object, the nondiagonal density matrix (in the position representation)

$$\left\{\begin{array}{c}\text{density}\\ \text{matrix}\end{array}\right\} : \rho(x,x',\beta) = \sum_n \psi_n(x)\mathrm{e}^{-\beta E_n}\psi_n^*(x'), \quad (3.5)$$

which is the central object of quantum statistics. For example, the partition function $Z(\beta)$ is the trace of the density matrix, i.e. the sum or the integral of its diagonal terms:

$$Z(\beta) = \mathrm{Tr}\ \rho = \int \mathrm{d}x\ \rho(x,x,\beta)\,. \quad (3.6)$$

We shall compute the density matrix in different settings, and often without knowing the eigenfunctions and eigenvalues. For the case of the harmonic oscillator, however, we have all that it takes to compute the density matrix from our solution of the Schrödinger equation (see Alg. 3.2 (`harmonic-density`) and Fig. 3.3). The output of this program will allow us to check less basic approaches.

Copyright © 2006. Oxford University Press, Incorporated. All rights reserved.

Krauth, Werner. Statistical Mechanics: Algorithms and Computations, Oxford University Press, Incorporated, 2006. ProQuest Ebook Central, http://ebookcentral.proquest.com/lib/tau/detail.action?docID=431021.
Created from tau on 2024-08-12 07:17:16.

procedure `harmonic-density`
input $\{\psi_0^{\text{h.o.}}(x), \ldots, \psi_N^{\text{h.o.}}(x)\}$ (from Alg. 3.1 (`harmonic-wavefunction`))
input $\{\psi_0^{\text{h.o.}}(x'), \ldots, \psi_N^{\text{h.o.}}(x')\}$
input $\{E_n = n + \frac{1}{2}\}$
$\rho^{\text{h.o.}}(x, x', \beta) \leftarrow 0$
for $n = 0, \ldots, N$ **do**
  $\{\ \rho^{\text{h.o.}}(x, x', \beta) \leftarrow \rho^{\text{h.o.}}(x, x', \beta) + \psi_n^{\text{h.o.}}(x)\psi_n^{\text{h.o.}}(x')\mathrm{e}^{-\beta E_n}$
output $\{\rho^{\text{h.o.}}(x, x', \beta)\}$

Algorithm 3.2 `harmonic-density`. Density matrix for the harmonic oscillator obtained from the lowest-energy wave functions (see eqn (3.5)).

3.1.2 Free density matrix

We move on to our first analytic calculation, a prerequisite for further developments: the density matrix of a free particle, with the Hamiltonian

$$H^{\text{free}}\psi = -\frac{1}{2}\frac{\partial^2}{\partial x^2}\psi = E\psi.$$

We put the particle in a box of length L with periodic boundary conditions, that is, a torus. The solutions of the Schrödinger equation in a periodic box are plane waves that are periodic in L:

$$\psi_n^{\text{a}}(x) = \sqrt{\frac{2}{L}}\sin\left(2n\pi\frac{x}{L}\right) \quad (n = 1, 2, \ldots), \tag{3.7}$$

$$\psi_n^{\text{s}}(x) = \sqrt{\frac{2}{L}}\cos\left(2n\pi\frac{x}{L}\right) (n = 0, 1, \ldots) \tag{3.8}$$

(see Fig. 3.4), where the superscripts denote wave functions that are antisymmetric and symmetric with respect to the center of the interval $[0, L]$. Equivalently, we can use complex wave functions

$$\psi_n^{\text{per},L}(x) = \sqrt{\frac{1}{L}}\exp\left(\mathrm{i}2n\pi\frac{x}{L}\right) \quad (n = -\infty, \ldots, \infty), \tag{3.9}$$

$$E_n = \frac{2n^2\pi^2}{L^2}, \tag{3.10}$$

which give

$$\begin{aligned}\rho^{\text{per},L}(x, x', \beta) &= \sum_n \psi_n^{\text{per},L}(x)\mathrm{e}^{-\beta E_n}\left[\psi_n^{\text{per},L}(x')\right]^* \\ &= \frac{1}{L}\sum_{n=-\infty}^{\infty}\exp\left[\mathrm{i}2\pi n\frac{x - x'}{L}\right]\exp\left(-\frac{\beta 2n^2\pi^2}{L^2}\right). \end{aligned} \tag{3.11}$$

We now let L tend to infinity (the exact expression for finite L is discussed in Subsection 3.1.3). In this limit, we can transform the sum in eqn (3.11) into an integral. It is best to introduce a dummy parameter

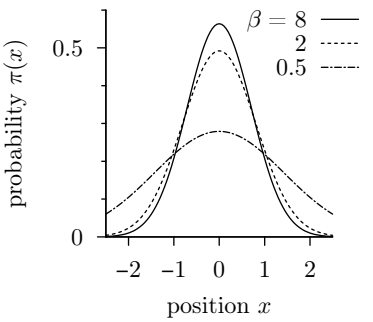

Fig. 3.3 Probability to be at position x, $\pi(x) = \rho^{\text{h.o.}}(x, x, \beta)/Z$ (from Alg. 3.2 (`harmonic-density`); see also eqn (3.39)).

Copyright © 2006. Oxford University Press, Incorporated. All rights reserved.

Krauth, Werner. Statistical Mechanics: Algorithms and Computations, Oxford University Press, Incorporated, 2006. ProQuest Ebook Central, http://ebookcentral.proquest.com/lib/tau/detail.action?docID=431021.
Created from tau on 2024-08-12 07:17:16.

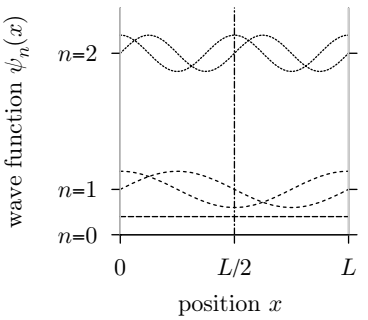

Fig. 3.4 Wave functions of a one-dimensional free particle in a torus of length L (shifted; see eqn (3.8)).

$\Delta_n = 1$, the difference between two successive n-values:

$$\rho^{\mathrm{per},L}(x,x',\beta) = \frac{1}{L}\sum_{n=-\infty}^{\infty} \overbrace{\Delta_n}^{=1} \exp\left[\mathrm{i}2n\pi\frac{x-x'}{L}\right] \exp\left(-\frac{\beta 2n^2\pi^2}{L^2}\right).$$

Changing variables from n to λ, where $\lambda = 2n\pi/L$, and thus $\Delta_\lambda = 2\pi\Delta_n/L$, gives the term-by-term equivalent sum

$$\rho^{\mathrm{per},L}(x,x',\beta) = \frac{1}{2\pi}\sum_{\lambda=\ldots,-\frac{2\pi}{L},0,\frac{2\pi}{L},\ldots} \Delta_\lambda \exp\left[\mathrm{i}\lambda(x-x')\right] \exp\left(-\frac{\beta}{2}\lambda^2\right)$$
$$\xrightarrow[L\to\infty]{} \frac{1}{2\pi}\int_{-\infty}^{\infty} \mathrm{d}\lambda\ \exp\left[\mathrm{i}\lambda(x-x')\right] \exp\left(-\frac{\beta}{2}\lambda^2\right).$$

This Gaussian integral can be evaluated (see eqn (3.12)). We arrive at the free density matrix, the periodic density matrix in the limit of an infinite torus:

$$\rho^{\mathrm{free}}(x,x',\beta) = \sqrt{\frac{m}{2\pi\hbar^2\beta}} \exp\left[-\frac{m(x-x')^2}{2\hbar^2\beta}\right], \tag{3.13}$$

where we have reinserted the Planck constant and the particle mass. In the limit of high temperature, $\rho^{\mathrm{free}}(x,x',\beta)$ is infinitely peaked at $x = x'$, and it continues to satisfy $\int_{-\infty}^{\infty} \mathrm{d}x\ \rho^{\mathrm{free}}(x,x',\beta) = 1$. This means that it realizes the Dirac δ-function:

$$\lim_{\beta\to 0} \rho^{\mathrm{free}}(x,x',\beta) \to \delta(x-x'). \tag{3.14}$$

For the perturbation theory of Subsection 3.2.1, we need the fact that the density matrix is generally given by the operator

$$\rho = \mathrm{e}^{-\beta H} = 1 - \beta H + \frac{1}{2}\beta^2 H^2 - \cdots. \tag{3.15}$$

We use

$$\int_{-\infty}^{\infty} \mathrm{d}\lambda\ \exp\left(-\frac{1}{2}\frac{\lambda^2}{\sigma^2} \pm \lambda\tilde{c}\right) = \sqrt{2\pi}\sigma \exp\left(\frac{1}{2}\tilde{c}^2\sigma^2\right), \tag{3.12}$$

which follows, when we take $\tilde{c} = c/\sigma^2$, from the Gaussian integral

$$\int_{-\infty}^{\infty} \frac{\mathrm{d}\lambda}{\sqrt{2\pi}\sigma} \exp\left[-\frac{1}{2}\frac{(\lambda\pm c)^2}{\sigma^2}\right] = 1.$$

Copyright © 2006. Oxford University Press, Incorporated. All rights reserved.

Krauth, Werner. Statistical Mechanics: Algorithms and Computations, Oxford University Press, Incorporated, 2006. ProQuest Ebook Central, http://ebookcentral.proquest.com/lib/tau/detail.action?docID=431021.
Created from tau on 2024-08-12 07:17:16.

The matrix elements of H in an arbitrary basis are $H_{kl} = \langle k|H|l\rangle$, and the matrix elements of ρ are

$$\langle k|\rho|l\rangle = \langle k|\mathrm{e}^{-\beta H}|l\rangle = \delta_{kl} - \beta H_{kl} + \frac{1}{2}\beta^2 \sum_n H_{kn}H_{nl} - \cdots .$$

Knowing the density matrix in any basis allows us to compute $\rho(x, x', \beta)$, i.e. the density matrix in the position representation:

$$\rho(x, x', \beta) = \sum_{kl} \underbrace{\langle x|k\rangle}_{\psi_k(x)} \langle k|\rho|l\rangle \underbrace{\langle l|x'\rangle}_{\psi_l^*(x')} .$$

This equation reduces to eqn (3.5) for the diagonal basis where $H_{nm} = E_n\delta_{nm}$ and $H_{nm}^2 = E_n^2\delta_{nm}$, etc.

3.1.3 Density matrices for a box

The density matrix $\rho(x, x', \beta)$ is as fundamental as the Boltzmann weight $\mathrm{e}^{-\beta E}$ of classical physics, but up to now we know it analytically only for the free particle (see eqn (3.13)). In the present subsection, we determine the density matrix of a free particle in a finite box, both with walls and with periodic boundary conditions. The two results will be needed in later calculations. For efficient simulations of a finite quantum system, say with periodic boundary conditions, it is better to start from the analytic solution of the noninteracting particle in a periodic box rather than from the free density matrix in the thermodynamic limit. (For the analytic expression of the density matrix for the harmonic oscillator, see Subsection 3.2.2.)

We first finish the calculation of the density matrix for a noninteracting particle with periodic boundary conditions, which we have evaluated only in the limit $L \to \infty$. We arrived in eqn (3.11) at the exact formula

$$\begin{aligned}\rho^{\mathrm{per},L}(x, x', \beta) &= \sum_{n=-\infty}^{\infty} \psi_n^{\mathrm{per},L}(x)\mathrm{e}^{-\beta E_n}\left[\psi_n^{\mathrm{per},L}(x')\right]^* \\ &= \frac{1}{L}\sum_{n=-\infty}^{\infty} \underbrace{\exp\left[\mathrm{i}2n\pi\frac{x-x'}{L}\right]\exp\left(-\frac{\beta n^2\pi^2}{L^2}\right)}_{g(n)} . \qquad (3.16)\end{aligned}$$

This infinite sum can be transformed using the Poisson sum formula

$$\sum_{n=-\infty}^{\infty} g(n) = \sum_{w=-\infty}^{\infty} \int_{-\infty}^{\infty} \mathrm{d}\phi\; g(\phi)\mathrm{e}^{\mathrm{i}2\pi w\phi} \qquad (3.17)$$

Copyright © 2006. Oxford University Press, Incorporated. All rights reserved.

Krauth, Werner. Statistical Mechanics: Algorithms and Computations, Oxford University Press, Incorporated, 2006. ProQuest Ebook Central, http://ebookcentral.proquest.com/lib/tau/detail.action?docID=431021.
Created from tau on 2024-08-12 07:17:16.

and the Gaussian integral rule (eqn (3.12)), to obtain

$$\underline{\rho^{\mathrm{per},L}(x,x',\beta)} = \sum_{w=-\infty}^{\infty} \int_{-\infty}^{\infty} \mathrm{d}\phi \, \exp\left(\mathrm{i}2\pi\phi \frac{x-x'+Lw}{L}\right) \exp\left(-\frac{\beta\pi^2\phi^2}{L^2}\right)$$
$$= \sqrt{\frac{1}{2\pi\beta}} \sum_{w=-\infty}^{\infty} \exp\left[-\frac{(x-x'-wL)^2}{2\beta}\right]$$
$$= \underline{\sum_{w=-\infty}^{\infty} \rho^{\mathrm{free}}(x,x'+wL,\beta)}. \quad (3.18)$$

The index w stands for the winding number in the context of periodic boundary conditions (see Subsection 2.1.4). The Poisson sum formula (eqn (3.17)) is itself derived as follows. For a function $g(\phi)$ that decays rapidly to zero at infinity, the periodic sum function $G(\phi) = \sum_{k=-\infty}^{\infty} g(\phi+k)$ can be expanded into a Fourier series:

$$G(\phi) = \underbrace{\sum_{k=-\infty}^{\infty} g(\phi+k)}_{\text{periodic in } [0,1]} = \sum_{w=-\infty}^{\infty} c_w \mathrm{e}^{\mathrm{i}2\pi w\phi}.$$

The Fourier coefficients $c_w = \int_0^1 \mathrm{d}\phi \; G(\phi)\mathrm{e}^{-\mathrm{i}2\pi w\phi}$ can be written as

$$c_w = \int_0^1 \mathrm{d}\phi \sum_{k=-\infty}^{\infty} g(\phi+k)\mathrm{e}^{-\mathrm{i}2\pi w\phi} = \int_{-\infty}^{\infty} \mathrm{d}\phi \; g(\phi)\mathrm{e}^{-\mathrm{i}2\pi w\phi}.$$

For $\phi = 0$, we obtain $G(0) = \sum_w c_w$, which gives eqn (3.17).

From eqn (3.18), we obtain the diagonal density matrix for a box with periodic boundary conditions as a sum over diagonal and nondiagonal free-particle density matrices:

$$\rho^{\mathrm{per},L}(x,x,\beta) = \sqrt{\frac{1}{2\pi\beta}} \left\{1 + \exp\left(-\frac{L^2}{2\beta}\right) + \exp\left[-\frac{(2L)^2}{2\beta}\right] + \cdots\right\}.$$

Using eqn (3.6), that is, integrating from 0 to L, we find a new expression for the partition function (see eqn (3.6)), differing in inspiration from the sum over energy eigenvalues but equivalent to it in outcome:

$$Z^{\mathrm{per},L} = \underbrace{\sum_{n=-\infty}^{\infty} \exp\left(-\beta\frac{2n^2\pi^2}{L^2}\right)}_{\text{sum over energy eigenvalues}} = \underbrace{\frac{L}{\sqrt{2\pi\beta}} \sum_{w=-\infty}^{\infty} \exp\left(-\frac{w^2L^2}{2\beta}\right)}_{\text{sum over winding numbers}}. \quad (3.19)$$

We next determine the density matrix of a free particle in a box of length L with hard walls rather than with periodic boundary conditions. Again, the free Hamiltonian is solved by plane waves, but they must vanish at $x = 0$ and at $x = L$:

$$\psi_n^{\mathrm{box},[0,\,L]}(x) = \sqrt{\frac{2}{L}} \sin\left(n\pi\frac{x}{L}\right) \quad (n = 1, \ldots, \infty) \quad (3.20)$$

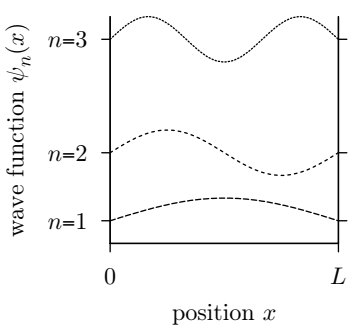

Fig. 3.5 Eigenfunctions of a one-dimensional free particle in a box (shifted); (see eqn (3.20), and compare with Fig. 3.4).

Copyright © 2006. Oxford University Press, Incorporated. All rights reserved.

Krauth, Werner. Statistical Mechanics: Algorithms and Computations, Oxford University Press, Incorporated, 2006. ProQuest Ebook Central, http://ebookcentral.proquest.com/lib/tau/detail.action?docID=431021.
Created from tau on 2024-08-12 07:17:16.

(see Fig. 3.5). The normalized and mutually orthogonal sine functions in eqn (3.20) have a periodicity $2L$, not L, unlike the wave functions in a box with periodic boundary conditions.

Using the plane waves in eqn (3.20) and their energies $E_n = \frac{1}{2}(n\pi/L)^2$, we find the following for the density matrix in the box:

$$\begin{aligned}\rho^{\mathrm{box},[0,\,L]}(x,x',\beta) &= \frac{2}{L}\sum_{n=1}^{\infty}\sin\left(\frac{\pi}{L}nx\right)\exp\left(-\beta\frac{\pi^2n^2}{2L^2}\right)\sin\left(\frac{\pi}{L}nx'\right)\\ &= \frac{1}{L}\sum_{n=-\infty}^{\infty}\sin\left(n\pi\frac{x}{L}\right)\exp\left(-\beta\frac{\pi^2n^2}{2L^2}\right)\sin\left(n\pi\frac{x'}{L}\right). \quad (3.21)\end{aligned}$$

We can write the product of the two sine functions as

$$\begin{aligned}&\sin\left(n\pi\frac{x}{L}\right)\sin\left(n\pi\frac{x'}{L}\right)\\ &\quad= \frac{1}{4}\left[\exp\left(in\pi\frac{x-x'}{L}\right)+\exp\left(-in\pi\frac{x-x'}{L}\right)\right.\\ &\qquad\left.-\exp\left(in\pi\frac{x+x'}{L}\right)-\exp\left(-in\pi\frac{x+x'}{L}\right)\right]. \quad (3.22)\end{aligned}$$

Using eqn (3.22) in eqn (3.21), and comparing the result with the formula for the periodic density matrix in eqn (3.11), which is itself expressed in terms of the free density matrix, we obtain

$$\begin{aligned}\underline{\rho^{\mathrm{box},[0,\,L]}(x,x',\beta)} &= \rho^{\mathrm{per},2L}(x,x',\beta)-\rho^{\mathrm{per},2L}(x,-x',\beta)\\ &= \underline{\sum_{w=-\infty}^{\infty}\left[\rho^{\mathrm{free}}(x,x'+2wL,\beta)-\rho^{\mathrm{free}}(x,-x'+2wL,\beta)\right]}. \quad (3.23)\end{aligned}$$

This intriguing sum over winding numbers is put together from terms different from those of eqn (3.21). It is, however, equivalent, as we can easily check in an example (see Fig. 3.6).

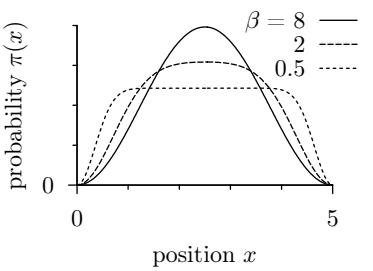

Fig. 3.6 Probability of being at position x for a free particle in a box with walls (from eqn (3.21) or eqn (3.23), with $L = 5$).

In conclusion, we have derived in this subsection the density matrix of a free particle in a box either with periodic boundary conditions or with walls. The calculations were done the hard way—explicit mathematics—using the Poisson sum formula and the representation of products of sine functions in terms of exponentials. The final formulas in eqns (3.18) and (3.23) can also be derived more intuitively, using path integrals, and they are more generally valid (see Subsection 3.3.3).

3.1.4 Density matrix in a rotating box

In Subsection 3.1.3, we determined the density matrix of a free quantum particle in a box with periodic boundary conditions. We now discuss the physical content of boundary conditions and the related counter-intuitive behavior of a quantum system under slow rotations. Our discussion is

Copyright © 2006. Oxford University Press, Incorporated. All rights reserved.

Krauth, Werner. Statistical Mechanics: Algorithms and Computations, Oxford University Press, Incorporated, 2006. ProQuest Ebook Central, http://ebookcentral.proquest.com/lib/tau/detail.action?docID=431021.
Created from tau on 2024-08-12 07:17:16.

a prerequisite for the treatment of superfluidity in quantum liquids (see Subsection 4.2.6), but also for superconductivity in electronic systems, a subject beyond the scope of this book.

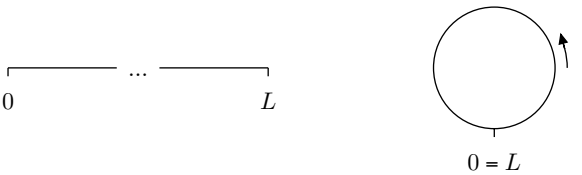

Fig. 3.7 A one-dimensional quantum system on a line of length L (*left*), and rolled up into a slowly rotating ring (*right*).

Let us imagine for a moment a complicated quantum system, for example a thin wire rolled up into a closed circle of circumference L, or a circular tube filled with a quantum liquid, ideally ^{4}He (see Fig. 3.7). Both systems are described by wave functions with periodic boundary conditions $\psi_n(0) = \psi_n(L)$. More precisely, the wave functions in the lab system for N conduction electrons or N helium atoms satisfy

$$\psi_n^{\rm lab}(x_1, \ldots, x_k + L, \ldots, x_N) = \psi_n^{\rm lab}(x_1, \ldots, x_k, \ldots, x_N). \qquad (3.24)$$

These boundary conditions for the wave functions in the laboratory frame continue to hold if the ring rotates with velocity v, because a quantum system—even if parts of it are moving—must be described everywhere by a single-valued wave function. The rotating system can be described in the laboratory reference frame using wave functions $\psi_n^{\rm lab}(x,t)$ and the time-dependent Hamiltonian $H^{\rm lab}(t)$, which represents the rotating crystal lattice or the rough surface of the tube enclosing the liquid.

The rotating system is more conveniently described in the corotating reference frame, using coordinates $x^{\rm rot}$ rather than the laboratory coordinates $x^{\rm lab}$ (see Table 3.1). In this reference frame, the crystal lattice or the container walls are stationary, so that the Hamiltonian $H^{\rm rot}$ is time independent. For very slow rotations, we can furthermore neglect centripetal forces and also magnetic fields generated by slowly moving charges. This implies that the Hamiltonian $H^{\rm rot}$ (with coordinates $x^{\rm rot}$) is the same as the laboratory Hamiltonian $H^{\rm lab}$ at $v = 0$. However, we shall see that the boundary conditions on the corotating wave functions $\psi^{\rm rot}$ are nontrivial.

To discuss this point, we now switch back from the complicated quantum systems to a free particle on a rotating ring, described by a Hamiltonian

$$H^{\rm rot} = -\frac{1}{2}\frac{\partial^2}{(\partial x^{\rm rot})^2}.$$

We shall go through the analysis of $H^{\rm rot}$, but keep in mind that the very distinction between rotating and laboratory frames is problematic for the

Table 3.1 Galilei transformation for a quantum system. $E^{\rm rot}$, $p_n^{\rm rot}$, and $x^{\rm rot}$ are defined in the moving reference frame.

Reference frame	
Lab.	Rot.
$x^{\rm lab} = x^{\rm rot} + vt$	$x^{\rm rot}$
$p_n^{\rm lab} = p_n^{\rm rot} + mv$	$p_n^{\rm rot}$
$E_n^{\rm lab} = \frac{1}{2m}(p_n^{\rm lab})^2$	$E_n^{\rm rot} = \frac{1}{2m}(p_n^{\rm rot})^2$

Copyright © 2006. Oxford University Press, Incorporated. All rights reserved.

Krauth, Werner. Statistical Mechanics: Algorithms and Computations, Oxford University Press, Incorporated, 2006. ProQuest Ebook Central, http://ebookcentral.proquest.com/lib/tau/detail.action?docID=431021.
Created from tau on 2024-08-12 07:17:16.

noninteracting system, because of the missing contact with the crystal lattice or the container boundaries. Strictly speaking, the distinction is meaningful for a noninteracting system only because the wave functions of the interacting system can be expanded in a plane-wave basis. In the rotating system, plane waves can be written as

$$\psi_n^{\rm rot}(x^{\rm rot}) = \exp\left(ip^{\rm rot}x^{\rm rot}\right).$$

This same plane wave can also be written, at all times, in the laboratory frame, where it must be periodic (see eqn (3.24)). The momentum of the plane wave in the laboratory system is related to that of the rotating system by the Galilei transform of Table 3.1.

$$p_n^{\rm lab} = \frac{2\pi}{L}n \implies p_n^{\rm rot} = \frac{2\pi}{L}n - mv \quad (n = -\infty, \ldots, \infty). \tag{3.25}$$

It follows from the Galilei transform of momenta and energies that the partition function $Z^{\rm rot}(\beta)$ in the rotating reference frame is

$$Z^{\rm rot}(\beta) = \sum_{n=-\infty}^{\infty} \exp\left[-\beta E_n^{\rm rot}\right] = \sum_{-\infty}^{\infty} \exp\left[-\frac{\beta}{2}\left(-v + 2n\pi/L\right)^2\right].$$

In the rotating reference frame, each plane wave with momentum $p_n^{\rm rot}$ contributes velocity $p_n^{\rm rot}/m$. The mean velocity measured in the rotating reference frame is

$$\left\langle v^{\rm rot}(\beta)\right\rangle = \frac{1}{mZ^{\rm rot}(\beta)} \sum_{n=-\infty}^{\infty} p_n^{\rm rot} \exp\left(-\beta E_n^{\rm rot}\right), \tag{3.26}$$

with energies and momenta given by eqn (3.25) that satisfy $E_n^{\rm rot} = (p_n^{\rm rot})^2/(2m)$. In the limit of zero temperature, only the lowest-lying state contributes to this rotating reference-frame particle velocity. The momentum of this state is generally nonzero, because the lowest energy state, the $n = 0$ state at very small rotation, $E_0^{\rm rot}$, has nonzero momentum (it corresponds to particle velocity $-v$). The particle velocity in the laboratory frame is

$$\left\langle v^{\rm lab}\right\rangle = \left\langle v^{\rm rot}\right\rangle + v. \tag{3.27}$$

At low temperature, this particle velocity differs from the velocity of the ring (see Fig. 3.8).

The particle velocity in a ring rotating with velocity v will now be obtained within the framework of density matrices, similarly to the way we obtained the density matrix for a stationary ring, in Subsection 3.1.3. Writing x for $x^{\rm rot}$ (they are the same at time $t = 0$, and we do not have to compare wave functions at different times),

$$\psi_n^{\rm rot}(x) = \sqrt{\frac{1}{L}} \exp\left(ip_n^{\rm rot}x\right) \qquad (n = -\infty, \ldots, \infty),$$
$$E_n^{\rm rot} = \frac{(p_n^{\rm rot})^2}{2m}.$$

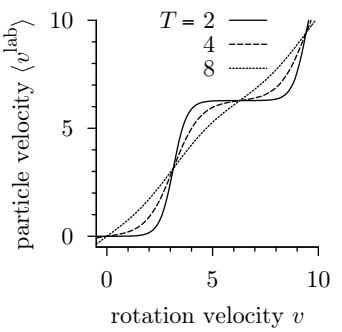

Fig. 3.8 Mean lab-frame velocity of a particle in a one-dimensional ring (from eqns (3.26) and (3.27) with $L = m = 1$).

Copyright © 2006. Oxford University Press, Incorporated. All rights reserved.

Krauth, Werner. Statistical Mechanics: Algorithms and Computations, Oxford University Press, Incorporated, 2006. ProQuest Ebook Central, http://ebookcentral.proquest.com/lib/tau/detail.action?docID=431021.
Created from tau on 2024-08-12 07:17:16.

The density matrix at positions x and x' in the rotating system is:

$$\rho^{\rm rot}(x,x',\beta) = \sum_{n=-\infty}^{\infty} {\rm e}^{-\beta E_n^{\rm rot}} \psi_n^{\rm rot}(x) \left[\psi_n^{\rm rot}(x')\right]^*$$
$$= \frac{1}{L} \sum_{n=-\infty}^{\infty} \underbrace{\exp\left[-\frac{\beta}{2}\left(p_n^{\rm rot}\right)^2\right] \exp\left[{\rm i}p_n^{\rm rot}\,(x-x')\right]}_{g(n),\ \text{compare with eqn (3.16)}}$$
$$= \sum_{w=-\infty}^{\infty} \int \frac{{\rm d}\phi}{L} \exp\left[-\frac{\beta}{2}\left(\frac{2\pi\phi}{L}-v\right)^2 + {\rm i}\left(\frac{2\pi\phi}{L}-v\right)(x-x') + {\rm i}2\pi w\phi\right],$$

where we have again used the Poisson sum formula (eqn (3.17)). Setting $\phi' = 2\pi\phi/L - v$ and changing w into $-w$, we reach

$$\rho^{\rm rot}(x,x',\beta) = \sum_{w=-\infty}^{\infty} {\rm e}^{-{\rm i}Lwv} \int_{-\infty}^{\infty} \frac{{\rm d}\phi}{2\pi} \exp\left[-\frac{\beta}{2}\phi'^2 + {\rm i}\phi'(x-x'-Lw)\right]$$
$$= \sum_{w=-\infty}^{\infty} {\rm e}^{-{\rm i}Lwv} \rho^{\rm free}(x,x'+Lw,\beta)\,.$$

Integrating the diagonal density matrix over all the positions x, from 0 to L, yields the partition function in the rotating system:

$$Z^{\rm rot}(\beta) = {\rm Tr}\,\rho^{\rm rot}(x,x,\beta)$$
$$= \sum_{w=-\infty}^{\infty} {\rm e}^{-{\rm i}Lvw} \int_0^L {\rm d}x\ \rho^{\rm free}(x,x+wL,\beta) \quad (3.28)$$

(see eqn (3.6)). For small velocities, we expand the exponential in the above equation. The zeroth-order term gives the partition function in the stationary system, and the first-order term vanishes because of a symmetry for the winding number $w \to -w$. The term proportional to w^2 is nontrivial. We multiply and divide by the laboratory partition function at rest, $Z_{v=0}^{\rm lab}$, and obtain

$$\underline{Z^{\rm rot}(\beta)} = \underbrace{\sum_{w=-\infty}^{\infty} \int_0^L {\rm d}x\ \rho^{\rm free}(x,x+wL,\beta)}_{Z_{v=0}^{\rm lab},\ \text{see eqn (3.18)}}$$
$$- \frac{1}{2}v^2L^2 \underbrace{\sum_{w=-\infty}^{\infty} \frac{w^2\rho^{\rm free}(x,x+wL,\beta)}{Z_{v=0}^{\rm lab}}}_{\langle w^2\rangle_{v=0}} Z_{v=0}^{\rm lab} + \cdots$$
$$= \underline{Z_{v=0}^{\rm lab}\left(1 - \frac{1}{2}v^2L^2\left\langle w^2\right\rangle_{v=0}\right)}.$$

Noting that the free energy is $F = -\log(Z)/\beta$, we obtain the following fundamental formula:

$$F^{\rm rot} = F_{v=0}^{\rm lab} + \frac{v^2L^2\left\langle w^2\right\rangle_{v=0}}{2\beta} + \cdots . \quad (3.29)$$

Copyright © 2006. Oxford University Press, Incorporated. All rights reserved.

Krauth, Werner. Statistical Mechanics: Algorithms and Computations, Oxford University Press, Incorporated, 2006. ProQuest Ebook Central, http://ebookcentral.proquest.com/lib/tau/detail.action?docID=431021.
Created from tau on 2024-08-12 07:17:16.

This is counter-intuitive because we would naively expect the slowly rotating system to rotate along with the reference system and have the same free energy as the laboratory system at rest, in the same way as a bucket of water, under very slow rotation, simply rotates with the walls and satisfies $F^{\rm rot} = F^{\rm lab}_{v=0}$. However, we saw the same effect in the previous calculation, using wave functions and eigenvalues. Part of the system simply does not rotate with the bucket. It remains stationary in the laboratory system.

The relation between the mean squared winding number and the change of free energies upon rotation is due to Pollock and Ceperley (1986). Equation (3.29) contains no more quantities specific to noninteracting particles; it therefore holds also in an interacting system, at least for small velocities. We shall understand this more clearly by representing the density matrix as a sum of paths, which do not change with interactions, and only get reweighted. Equation (3.29) is very convenient for evaluating the superfluid fraction of a liquid, that part of a very slowly rotating system which remains stationary in the laboratory frame.

In conclusion, we have computed in this subsection the density matrix for a free particle in a rotating box. As mentioned several times, this calculation has far-reaching consequences for quantum liquids and superconductors. Hess and Fairbank (1967) demonstrated experimentally that a quantum liquid in a slowly rotating container rotates more slowly than the container, or even stops to rest. The reader is urged to study the experiment, and Leggett's classic discussion (Leggett 1973).

3.2 Matrix squaring

A classical equilibrium system is at coordinates $\mathbf{x}$ with a probability $\pi(\mathbf{x})$ given by the Boltzmann distribution. In contrast, a quantum statistical system is governed by the diagonal density matrix, defined through wave functions and energy eigenvalues. The problem is that we usually do not know the solutions of the Schrödinger equation, so that we need other methods to compute the density matrix. In this section, we discuss matrix squaring, an immensely practical approach to computing the density matrix at any temperature from a high-temperature limit with the help of a convolution principle, which yields the density matrix at low temperature once we know it at high temperature.

Convolutions of probability distributions have already been discussed in Chapter 1. Their relation to convolutions of density matrices will become evident in the context of the Feynman path integral (see Section 3.3).

3.2.1 High-temperature limit, convolution

In the limit of high temperature, the density matrix of a quantum system described by a Hamiltonian $H = H^{\rm free} + V$ is given by a general

Copyright © 2006. Oxford University Press, Incorporated. All rights reserved.

Krauth, Werner. Statistical Mechanics: Algorithms and Computations, Oxford University Press, Incorporated, 2006. ProQuest Ebook Central, http://ebookcentral.proquest.com/lib/tau/detail.action?docID=431021.
Created from tau on 2024-08-12 07:17:16.

expression known as the Trotter formula:

$$\rho(x,x',\beta) \xrightarrow[\beta\to 0]{} \mathrm{e}^{-\frac{1}{2}\beta V(x)}\rho^{\mathrm{free}}(x,x',\beta)\ \mathrm{e}^{-\frac{1}{2}\beta V(x')}. \tag{3.30}$$

To verify eqn (3.30), we expand the exponentials of operators, but observe that terms may not commute, that is, $H_{\mathrm{free}}V \neq VH_{\mathrm{free}}$. We then compare the result with the expansion in eqn (3.15) of the density matrix $\rho = \mathrm{e}^{-\beta H}$. The above Trotter formula gives

$$\left(1-\underbrace{\frac{\beta}{2}V}_{a}+\underbrace{\frac{\beta^2}{8}V^2}_{b}\ldots\right)\left[1-\underbrace{\beta H^{\mathrm{free}}}_{c}+\underbrace{\frac{\beta^2}{2}(H^{\mathrm{free}})^2}_{d}\ldots\right]\left(1-\underbrace{\frac{\beta}{2}V}_{e}+\underbrace{\frac{\beta^2}{8}V^2}_{f}\ldots\right),$$

which yields

$$1-\underbrace{\beta(V+H^{\mathrm{free}})}_{a+e+c}+\frac{\beta^2}{2}\Big[\underbrace{V^2}_{ae+b+f}+\underbrace{VH^{\mathrm{free}}}_{ac}+\underbrace{H^{\mathrm{free}}V}_{ce}+\underbrace{(H^{\mathrm{free}})^2}_{d}\Big]-\cdots.$$

This agrees up to order β^2 with the expansion of

$$\mathrm{e}^{-\beta(V+H^{\mathrm{free}})} = 1-\beta(V+H^{\mathrm{free}})+\frac{\beta^2}{2}\underbrace{(V+H^{\mathrm{free}})(V+H^{\mathrm{free}})}_{V^2+VH^{\mathrm{free}}+H^{\mathrm{free}}V+(H^{\mathrm{free}})^2}+\cdots.$$

The above manipulations are generally well defined for operators and wave functions in a finite box.

Any density matrix $\rho(x,x',\beta)$ possesses a fundamental convolution property:

$$\underline{\int \mathrm{d}x'\ \rho(x,x',\beta_1)\,\rho(x',x'',\beta_2)} \tag{3.31}$$

$$= \int \mathrm{d}x' \sum_{n,m}\psi_n(x)\mathrm{e}^{-\beta_1 E_n}\psi_n^*(x')\psi_m(x')\mathrm{e}^{-\beta_2 E_m}\psi_m^*(x'')$$

$$= \sum_{n,m}\psi_n(x)\mathrm{e}^{-\beta_1 E_n}\underbrace{\int \mathrm{d}x'\ \psi_n^*(x')\psi_m(x')}_{\delta_{nm},\ \text{see eqn (3.2)}}\mathrm{e}^{-\beta_2 E_m}\psi_m^*(x'')$$

$$= \sum_n \psi_n(x)\mathrm{e}^{-(\beta_1+\beta_2)E_n}\psi_n^*(x'') = \underline{\rho(x,x'',\beta_1+\beta_2)}. \tag{3.32}$$

We can thus express the density matrix in eqn (3.32) at the inverse temperature $\beta_1+\beta_2$ (low temperature) as an integral (eqn (3.31)) over density matrices at higher temperatures corresponding to β_1 and β_2. Let us suppose that the two temperatures are the same ($\beta_1=\beta_2=\beta$) and that the positions x are discretized. The integral in eqn (3.31) then turns into a sum $\sum_l$, and $\rho(x,x',\beta)$ becomes a discrete matrix ρ_{kl}. The convolution turns into a product of a matrix with itself, a matrix squared:

$$\begin{array}{ccccc} \int \mathrm{d}x'\ \rho(x,x',\beta)\ \rho(x',x'',\beta) & = & \rho(x,x'',2\beta)\,. \\ \Updownarrow & & \Updownarrow & & \Updownarrow \\ \sum_l \quad \rho_{kl} & & \rho_{lm} & = & \left(\rho^2\right)_{km} \end{array}$$

Copyright © 2006. Oxford University Press, Incorporated. All rights reserved.

Krauth, Werner. Statistical Mechanics: Algorithms and Computations, Oxford University Press, Incorporated, 2006. ProQuest Ebook Central, http://ebookcentral.proquest.com/lib/tau/detail.action?docID=431021.
Created from tau on 2024-08-12 07:17:16.

Matrix squaring was first applied by Storer (1968) to the convolution of density matrices. It can be iterated: after computing the density matrix at 2β, we go to 4β, then to 8β, etc., that is, to lower and lower temperatures. Together with the Trotter formula, which gives a high-temperature approximation, we thus have a systematic procedure for computing the low-temperature density matrix. The procedure works for any Hamiltonian provided we can evaluate the integral in eqn (3.31) (see Alg. 3.3 (`matrix-square`)). We need not solve for eigenfunctions and eigenvalues of the Schrödinger equation. To test the program, we may iterate Alg. 3.3 (`matrix-square`) several times for the harmonic oscillator, starting from the Trotter formula at high temperature. With some trial and error to determine a good discretization of x-values and a suitable initial temperature, we can easily recover the plots of Fig. 3.3.

procedure `matrix-square`
input $\{x_0, \ldots, x_K\}, \{\rho(x_k, x_l, \beta)\}$ (grid with step size Δ_x)
for $x = x_0, \ldots, x_K$ **do**
  { **for** $x' = x_0, \ldots, x_K$ **do**
    { $\rho(x, x', 2\beta) \leftarrow \sum_k \Delta_x \rho(x, x_k, \beta)\, \rho(x_k, x', \beta)$
output $\{\rho(x_k, x_l, 2\beta)\}$

Algorithm 3.3 `matrix-square`. Density matrix at temperature $1/(2\beta)$ obtained from that at $1/\beta$ by discretizing the integral in eqn (3.32).

3.2.2 Harmonic oscillator (exact solution)

Quantum-statistics problems can be solved by plugging the high-temperature approximation for the density matrix into a matrix-squaring routine and iterating down to low temperature (see Subsection 3.2.1). This strategy works for anything from the simplest test cases to complicated quantum systems in high spatial dimensions, interacting particles, bosons, fermions, etc. How we actually do the integration inside the matrix-squaring routine depends on the specific problem, and can involve saddle point integration or other approximations, Riemann sums, Monte Carlo sampling, etc. For the harmonic oscillator, all the integrations can be done analytically. This yields an explicit formula for the density matrix for a harmonic oscillator at arbitrary temperature, which we shall use in later sections and chapters.

The density matrix at high temperature,

$$\rho^{\text{h.o.}}(x, x', \beta) \xrightarrow[\beta \to 0]{\text{from eqn (3.30)}} \sqrt{\frac{1}{2\pi\beta}} \exp\left[-\frac{\beta}{4}x^2 - \frac{(x-x')^2}{2\beta} - \frac{\beta}{4}x'^2\right],$$

can be written as

$$\rho^{\text{h.o.}}(x, x', \beta) = c(\beta) \exp\left[-g(\beta)\frac{(x-x')^2}{2} - f(\beta)\frac{(x+x')^2}{2}\right], \quad (3.33)$$

Copyright © 2006. Oxford University Press, Incorporated. All rights reserved.

Krauth, Werner. Statistical Mechanics: Algorithms and Computations, Oxford University Press, Incorporated, 2006. ProQuest Ebook Central, http://ebookcentral.proquest.com/lib/tau/detail.action?docID=431021.
Created from tau on 2024-08-12 07:17:16.

where

$$\begin{aligned} f(\beta) &\xrightarrow[\beta\to 0]{} \frac{\beta}{4}, \\ g(\beta) &\xrightarrow[\beta\to 0]{} \frac{1}{\beta}+\frac{\beta}{4}, \\ c(\beta) &\xrightarrow[\beta\to 0]{} \sqrt{\frac{1}{2\pi\beta}}. \end{aligned} \tag{3.34}$$

The convolution of two Gaussians is again a Gaussian, so that the harmonic-oscillator density matrix at inverse temperature 2β,

$$\rho^{\text{h.o.}}(x,x'',2\beta)=\int_{-\infty}^{\infty}\mathrm{d}x'\;\rho^{\text{h.o.}}(x,x',\beta)\,\rho^{\text{h.o.}}(x',x'',\beta)\,,$$

must also have the functional form of eqn (3.33). We recast the exponential in the above integrand,

$$\begin{aligned} &-\frac{f}{2}\left[(x+x')^2+(x'+x'')^2\right]-\frac{g}{2}\left[(x-x')^2+(x'-x'')^2\right] \\ &\qquad=\underbrace{-\frac{f+g}{2}\left(x^2+x''^2\right)}_{\text{independent of } x'}\;\underbrace{-2(f+g)\frac{x'^2}{2}-(f-g)(x+x'')x'}_{\text{Gaussian in } x',\ \text{variance } \sigma^2=(2f+2g)^{-1}}, \end{aligned}$$

and obtain, using eqn (3.12),

$$\begin{aligned} &\rho^{\text{h.o.}}(x,x'',2\beta) \\ &\qquad=c(2\beta)\exp\left[-\frac{f+g}{2}\left(x^2+x''^2\right)+\frac{1}{2}\frac{(f-g)^2}{f+g}\frac{(x+x'')^2}{2}\right]. \end{aligned} \tag{3.35}$$

The argument of the exponential function in eqn (3.35) is

$$-\underbrace{\left[\frac{f+g}{2}-\frac{1}{2}\frac{(f-g)^2}{f+g}\right]}_{f(2\beta)}\frac{(x+x'')^2}{2}-\underbrace{\left(\frac{f+g}{2}\right)}_{g(2\beta)}\frac{(x-x'')^2}{2}.$$

We thus find

$$\begin{aligned} f(2\beta)&=\frac{f(\beta)+g(\beta)}{2}-\frac{1}{2}\frac{[f(\beta)-g(\beta)]^2}{f(\beta)+g(\beta)}=\frac{2f(\beta)g(\beta)}{f(\beta)+g(\beta)}, \\ g(2\beta)&=\frac{f(\beta)+g(\beta)}{2}, \\ c(2\beta)&=c^2(\beta)\sqrt{\frac{2\pi}{2[f(\beta)+g(\beta)]}}=c^2(\beta)\frac{\sqrt{2\pi}}{2\sqrt{g(2\beta)}}. \end{aligned}$$

The recursion relations for f and g imply

$$f(2\beta)g(2\beta)=f(\beta)g(\beta)=f(\beta/2)g(\beta/2)=\cdots=\frac{1}{4},$$

Copyright © 2006. Oxford University Press, Incorporated. All rights reserved.

Krauth, Werner. Statistical Mechanics: Algorithms and Computations, Oxford University Press, Incorporated, 2006. ProQuest Ebook Central, http://ebookcentral.proquest.com/lib/tau/detail.action?docID=431021.
Created from tau on 2024-08-12 07:17:16.

because of the high-temperature limit in eqn (3.34), and therefore

$$g(2\beta) = \frac{g(\beta) + (1/4)g^{-1}(\beta)}{2}. \tag{3.36}$$

We can easily check that the only function satisfying eqn (3.36) with the limit in eqn (3.34) is

$$g(\beta) = \frac{1}{2}\coth\frac{\beta}{2} \implies f(\beta) = \frac{1}{2}\tanh\frac{\beta}{2}.$$

Knowing $g(\beta)$ and thus $g(2\beta)$, we can solve for $c(\beta)$ and arrive at

$$\rho^{\text{h.o.}}(x, x', \beta) = \sqrt{\frac{1}{2\pi\sinh\beta}}\exp\left[-\frac{(x+x')^2}{4}\tanh\frac{\beta}{2} - \frac{(x-x')^2}{4}\coth\frac{\beta}{2}\right], \tag{3.37}$$

and the diagonal density matrix is

$$\rho^{\text{h.o.}}(x, x, \beta) = \sqrt{\frac{1}{2\pi\sinh\beta}}\exp\left(-x^2\tanh\frac{\beta}{2}\right). \tag{3.38}$$

To introduce physical units into these two equations, we must replace

$$x \to \sqrt{\frac{m\omega}{\hbar}}x,$$
$$\beta \to \hbar\omega\beta = \frac{\hbar\omega}{k_{\text{B}}T},$$

and also multiply the density matrix by a factor $\sqrt{m\omega/\hbar}$.

We used Alg. 3.2 (`harmonic-density`) earlier to compute the diagonal density matrix $\rho^{\text{h.o.}}(x, x, \beta)$ from the wave functions and energy eigenvalues. We now see that the resulting plots, shown in Fig. 3.3, are simply Gaussians of variance

$$\sigma^2 = \frac{1}{2\tanh(\beta/2)}. \tag{3.39}$$

For a classical harmonic oscillator, the analogous probabilities are obtained from the Boltzmann distribution

$$\pi^{\text{class.}}(x) \propto \mathrm{e}^{-\beta E(x)} = \exp\left(-\beta x^2/2\right).$$

This is also a Gaussian, but its variance ($\sigma^2 = 1/\beta$) agrees with that in the quantum problem only in the high-temperature limit (see eqn (3.39) for $\beta \to 0$). Integrating the diagonal density matrix over space gives the partition function of the harmonic oscillator:

$$Z^{\text{h.o.}}(\beta) = \int \mathrm{d}x\ \rho^{\text{h.o.}}(x, x, \beta) = \frac{1}{2\sinh(\beta/2)}, \tag{3.40}$$

where we have used the fact that

$$\tanh\frac{\beta}{2}\sinh\beta = 2\left(\sinh\frac{\beta}{2}\right)^2.$$

Copyright © 2006. Oxford University Press, Incorporated. All rights reserved.

Krauth, Werner. Statistical Mechanics: Algorithms and Computations, Oxford University Press, Incorporated, 2006. ProQuest Ebook Central, http://ebookcentral.proquest.com/lib/tau/detail.action?docID=431021.
Created from tau on 2024-08-12 07:17:16.

This way of computing the partition function agrees with what we obtained from the sum of energies in eqn (3.3). Matrix squaring also allows us to compute the ground-state wave function without solving the Schrödinger equation because, in the limit of zero temperature, eqn (3.38) becomes $\rho^{\text{h.o.}}(x,x,\beta) \propto \exp\left(-x^2\right) \propto \psi_0^{\text{h.o.}}(x)^2$ (see Alg. 3.1 (`harmonic-wavefunction`)).

In conclusion, we have obtained in this subsection an analytic expression for the density matrix of a harmonic oscillator, not from the energy eigenvalues and eigenfunctions, but using matrix squaring down from high temperature. We shall need this expression several times in this chapter and in Chapter 4.

3.2.3 Infinitesimal matrix products

The density matrix at low temperature (inverse temperature $\beta_1 + \beta_2$) $\rho(x,x',\beta_1+\beta_2)$ is already contained in the density matrices at β_1 and β_2. We can also formulate this relation between density matrices at two different temperatures in terms of a differential relation, by taking one of the temperatures to be infinitesimally small:

$$\rho(\Delta\beta)\rho(\beta) = \rho(\beta+\Delta\beta).$$

Because of $\rho(\Delta\beta) = \mathrm{e}^{-\Delta\beta H} \simeq 1 - \Delta\beta H$, this is equivalent to

$$\underline{-H\rho} \simeq \frac{\rho(\beta+\Delta\beta)-\rho(\beta)}{\Delta\beta} = \underline{\frac{\partial}{\partial\beta}\rho}. \tag{3.41}$$

The effect of the hamiltonian on the density matrix is best clarified in the position representation, where one finds, either by inserting complete sets of states into eqn (3.41) or from the definition of the density matrix:

$$\frac{\partial}{\partial\beta}\rho(x,x',\beta) = -\sum_n \underbrace{E_n\psi_n(x)}_{H\psi_n(x)} \mathrm{e}^{-\beta E_n}\psi_n^*(x') = -H_x\rho(x,x',\beta)\,, \tag{3.42}$$

where H_x means that the Hamiltonian acts on x, not on x', in the density matrix $\rho(x,x',\beta)$. Equation (3.42) is the differential version of matrix squaring, and has the same initial condition at infinite temperature: $\rho(x,x',\beta\to 0) \to \delta(x-x')$ (see eqn (3.14)).

We shall not need the differential equation (3.42) in the further course of this book and shall simply check in passing that it is satisfied by $\rho^{\text{free}}(x,x',\beta)$. We have

$$\begin{aligned}\frac{\partial}{\partial\beta}\rho^{\text{free}}(x,x',\beta) &= \frac{\partial}{\partial\beta}\left\{\frac{1}{\sqrt{2\pi\beta}}\exp\left[-\frac{(x-x')^2}{2\beta}\right]\right\} \\ &= \frac{-\beta+(x-x')^2}{2\beta^2}\rho^{\text{free}}(x,x',\beta)\,.\end{aligned}$$

On the other hand, we can explicitly check that:

$$\frac{\partial^2}{\partial x^2}\rho^{\text{free}}(x,x',\beta) = \rho^{\text{free}}(x,x',\beta)\,\frac{(x-x')^2}{\beta^2} - \rho^{\text{free}}(x,x',\beta)\,/\beta,$$

Copyright © 2006. Oxford University Press, Incorporated. All rights reserved.

Krauth, Werner. Statistical Mechanics: Algorithms and Computations, Oxford University Press, Incorporated, 2006. ProQuest Ebook Central, http://ebookcentral.proquest.com/lib/tau/detail.action?docID=431021.
Created from tau on 2024-08-12 07:17:16.

so that the free density matrix solves the differential equation (3.42).

In this book, we shall be interested only in the density matrix in statistical mechanics, shown in eqn (3.41), which is related to the evolution operator in real time, $\mathrm{e}^{-\mathrm{i}tH}$. Formally, we can pass from real time t to inverse temperature β through the replacement

$$\beta = \mathrm{i}t,$$

and β is often referred to as an "imaginary" time. The quantum Monte Carlo methods in this chapter and in Chapter 4 usually do not carry over to real-time quantum dynamics, because the weights would become complex numbers, and could then no longer be interpreted as probabilities.

3.3 The Feynman path integral

In matrix squaring, one of the subjects of Section 3.2, we convolute two density matrices at temperature T to produce the density matrix at temperature $T/2$. By iterating this process, we can obtain the density matrix at any temperature from the quasi-classical high-temperature limit. Most often, however, it is impossible to convolute two density matrices analytically. With increasing numbers of particles and in high dimensionality, the available computer memory soon becomes insufficient even to store a reasonably discretized matrix $\rho(\mathbf{x}, \mathbf{x}', \beta)$, so that one cannot run Alg. 3.3 (`matrix-square`) on a discretized approximation of the density matrix. Monte Carlo methods are able to resolve this problem. They naturally lead to the Feynman path integral for quantum systems and to the idea of path sampling, as we shall see in the present section.

Instead of evaluating the convolution integrals one after the other, as is done in matrix squaring, we can write them out all together:

$$\begin{aligned}\rho(x, x', \beta) &= \int \mathrm{d}x''\ \rho(x, x'', \beta/2)\, \rho(x'', x', \beta/2) \\ &= \iiint \mathrm{d}x''\mathrm{d}x'''\mathrm{d}x''''\rho(x, x''', \frac{\beta}{4})\, \rho(x''', x'', \frac{\beta}{4})\, \rho(x'', x'''', \frac{\beta}{4})\, \rho(x'''', x', \frac{\beta}{4}) \\ &= \dots.\end{aligned}$$

This equation continues to increasingly deeper levels, with the kth applications of the matrix-squaring algorithm corresponding to $\simeq 2^k$ integrations. Writing $\{x_0, x_1, \dots\}$ instead of the cumbersome $\{x, x', x'', \dots\}$, this gives

$$\begin{aligned}\rho(x_0, x_N, \beta) = \int \cdots \int \mathrm{d}x_1 \dots \mathrm{d}x_{N-1} \\ \times \rho\left(x_0, x_1, \frac{\beta}{N}\right) \dots \rho\left(x_{N-1}, x_N, \frac{\beta}{N}\right), \quad (3.43)\end{aligned}$$

where we note that, for the density matrix $\rho(x_0, x_N, \beta)$, the variables x_0 and x_N are fixed on both sides of eqn (3.43). For the partition function,

Copyright © 2006. Oxford University Press, Incorporated. All rights reserved.

Krauth, Werner. Statistical Mechanics: Algorithms and Computations, Oxford University Press, Incorporated, 2006. ProQuest Ebook Central, http://ebookcentral.proquest.com/lib/tau/detail.action?docID=431021.
Created from tau on 2024-08-12 07:17:16.

there is one more integration, over the variable x_0, which is identified with x_N:

$$Z = \int \mathrm{d}x_0 \; \rho(x_0, x_0, \beta) = \int \cdots \int \mathrm{d}x_0 \ldots \mathrm{d}x_{N-1} \times \rho\left(x_0, x_1, \frac{\beta}{N}\right) \ldots \rho\left(x_{N-1}, x_0, \frac{\beta}{N}\right). \quad (3.44)$$

The sequence $\{x_0, \ldots, x_N\}$ in eqns (3.43) and (3.44) is called a path, and we can imagine the variable x_k at the value $k\beta/N$ of the imaginary-time variable τ, which goes from 0 to β in steps of $\Delta_\tau = \beta/N$ (see Feynman (1972)). Density matrices and partition functions are thus represented as multiple integrals over paths, called path integrals, both at finite N and in the limit $N \to \infty$. The motivation for this representation is again that for large N, the density matrices under the multiple integral signs are at small $\Delta_\tau = \beta/N$ (high temperature) and can thus be replaced by their quasi-classical high-temperature approximations. To distinguish between the density matrix with fixed positions x_0 and x_N and the partition function, where one integrates over $x_0 = x_N$, we shall refer to the paths in eqn (3.43) as contributing to the density matrix $\rho(x_0, x_N, \beta)$, and to the paths in eqn (3.44) as contributing to the partition function.

After presenting a naive sampling approach in Subsection 3.3.1, we discuss direct path sampling using the Lévy construction, in Subsection 3.3.2. The closely related later Subsection 3.5.1 introduces path sampling in Fourier space.

3.3.1 Naive path sampling

The Feynman path integral describes a single quantum particle in terms of paths $\{x_0, \ldots, x_N\}$ (often referred to as world lines), with weights given by the high-temperature density matrix or another suitable approximation:

$$Z = \underbrace{\int \int \mathrm{d}x_0, \ldots, \mathrm{d}x_{N-1}}_{\text{sum of paths}} \underbrace{\rho(x_0, x_1, \Delta_\tau) \cdot \cdots \cdot \rho(x_{N-1}, x_0, \Delta_\tau)}_{\text{weight } \pi \text{ of path}}.$$

More generally, any variable x_k can represent a d-dimensional quantum system. The full path then lies in $d+1$ dimensions.

Let us first sample the paths contributing to the partition function of a harmonic oscillator using a local Markov-chain algorithm (see Fig. 3.9). We implement the Trotter formula, as we would for an arbitrary potential. Each path comes with a weight containing terms as the following:

$$\underbrace{\ldots \rho^{\text{free}}(x_{k-1}, x_k, \Delta_\tau)\, \mathrm{e}^{-\frac{1}{2}\Delta_\tau V(x_k)}}_{\rho(x_{k-1}, x_k, \Delta_\tau) \text{ in Trotter formula}} \underbrace{\mathrm{e}^{-\frac{1}{2}\Delta_\tau V(x_k)} \rho^{\text{free}}(x_k, x_{k+1}, \Delta_\tau) \ldots}_{\rho(x_k, x_{k+1}, \Delta_\tau) \text{ in Trotter formula}}.$$

As shown, each argument x_k appears twice, and any two contributions $\exp\left[-\frac{1}{2}\Delta_\tau V(x_k)\right]$, where $V(x) = \frac{1}{2}x^2$, can be combined into a single

Copyright © 2006. Oxford University Press, Incorporated. All rights reserved.

Krauth, Werner. Statistical Mechanics: Algorithms and Computations, Oxford University Press, Incorporated, 2006. ProQuest Ebook Central, http://ebookcentral.proquest.com/lib/tau/detail.action?docID=431021.
Created from tau on 2024-08-12 07:17:16.

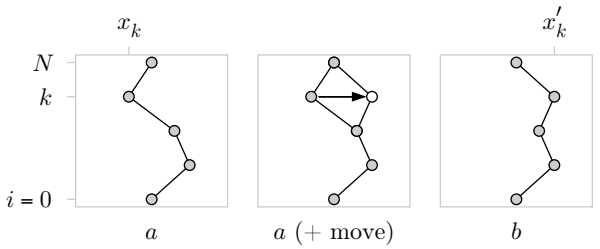

Fig. 3.9 Naive path-sampling move. The ratio π_b/π_a is computed from $\{x_{k-1}, x_k, x_{k+1}\}$ and from the new position x'_k.

term $\exp[-\Delta_\tau V(x_k)]$. To move from one position of the path to the next, we choose a random element k and accept the move $x_k \to x_k + \delta_x$ using the Metropolis algorithm. The ratio of the weights of the new and the old path involves only two segments of the path and one interaction potential (see Alg. 3.4 (`naive-harmonic-path`)). A move of x_k, for $k \neq 0$, involves segments $\{x_{k-1}, x_k\}$ and $\{x_k, x_{k+1}\}$. Periodic boundary conditions in the τ-domain have been worked in: for $k = 0$, we consider the density matrices between $\{x_{N-1}, x_0\}$ and $\{x_0, x_1\}$. Such a move across the horizon $k = 0$ changes x_0 and x_N, but they are the same (see the iteration $i = 10$ in Fig. 3.11).

procedure `naive-harmonic-path`
input $\{x_0, \ldots, x_{N-1}\}$
$\Delta_\tau \leftarrow \beta/N$
$k \leftarrow \texttt{nran}\,(0, N-1)$
$k_\pm \leftarrow k \pm 1$
if $(k_- = -1) k_- \leftarrow N$
$x'_k \leftarrow x_k + \texttt{ran}\,(-\delta, \delta)$
$\pi_a \leftarrow \rho^{\text{free}}(x_{k_-}, x_k, \Delta_\tau)\, \rho^{\text{free}}(x_k, x_{k_+}, \Delta_\tau) \exp\left(-\frac{1}{2}\Delta_\tau x_k^2\right)$
$\pi_b \leftarrow \rho^{\text{free}}(x_{k_-}, x'_k, \Delta_\tau)\, \rho^{\text{free}}(x'_k, x_{k_+}, \Delta_\tau) \exp\left(-\frac{1}{2}\Delta_\tau x_k'^2\right)$
$\Upsilon \leftarrow \pi_b/\pi_a$
if $(\texttt{ran}\,(0,1) < \Upsilon) x_k \leftarrow x'_k$
output $\{x_0, \ldots, x_{N-1}\}$

Algorithm 3.4 `naive-harmonic-path`. Markov-chain sampling of paths contributing to $Z^{\text{h.o.}} = \int \mathrm{d}x_0\ \rho^{\text{h.o.}}(x_0, x_0, \beta)$.

Algorithm 3.4 (`naive-harmonic-path`) is an elementary path-integral Monte Carlo program. To test it, we can generate a histogram of positions for any of the x_k (see Fig. 3.10). For large N, the error in the Trotter formula is negligible. The histogram must then agree with the analytical result for the probability $\pi(x) = \rho^{\text{h.o.}}(x, x, \beta)/Z$, which we can also calculate from eqns (3.38) and (3.40). This simple path-integral

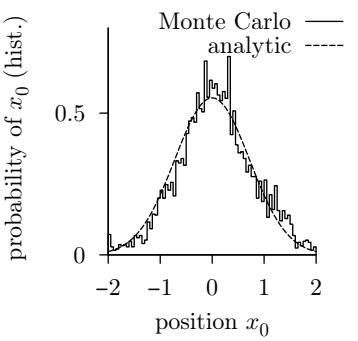

Fig. 3.10 Histogram of positions x_0 (from Alg. 3.4 (`naive-harmonic-path`), with $\beta = 4$, $N = 8$, and 1×10^6 iterations).

Copyright © 2006. Oxford University Press, Incorporated. All rights reserved.

Krauth, Werner. Statistical Mechanics: Algorithms and Computations, Oxford University Press, Incorporated, 2006. ProQuest Ebook Central, http://ebookcentral.proquest.com/lib/tau/detail.action?docID=431021.
Created from tau on 2024-08-12 07:17:16.

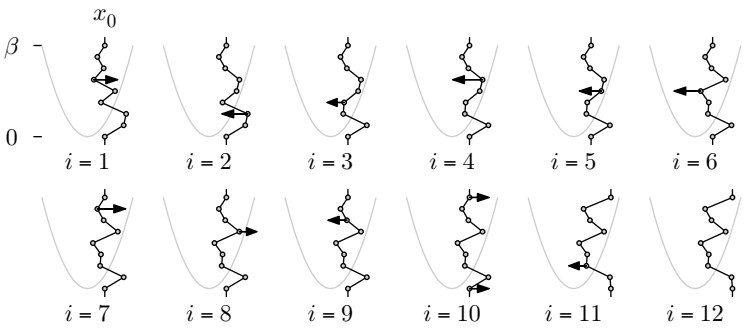

Fig. 3.11 Markov-chain path sampling for a harmonic potential (from Alg. 3.4 (`naive-harmonic-path`)).

Monte Carlo program can in principle, but rarely in practice, solve problems in equilibrium quantum statistical physics.

Algorithm 3.4 (`naive-harmonic-path`), like local path sampling in general, is exceedingly slow. This can be seen from the fluctuations in the histogram in Fig. 3.10 or in the fact that the path positions in Fig. 3.11 are all on the positive side ($x_k > 0$), just as in the initial configuration: Evidently, a position x_k cannot get too far away from x_{k-1} and x_{k+1}, because the free density matrix then quickly becomes very small. Local path sampling is unfit for complicated problems.

3.3.2 Direct path sampling and the Lévy construction

To overcome the limitations of local path sampling, we must analyze the origin of the high rejection rate. As discussed in several other places in this book, a high rejection rate signals an inefficient Monte Carlo algorithm, because it forces us to use small displacements δ. This is what happens in Alg. 3.4 (`naive-harmonic-path`). We cannot move x_k very far away from its neighbors, and are also prevented from moving larger parts of the path, consisting of positions $\{x_k, \ldots, x_{k+l}\}$. For concreteness, we first consider paths contributing to the density matrix of a free particle, and later on the paths for the harmonic oscillator. Let us sample the integral

$$\rho^{\text{free}}(x_0, x_N, \beta) = \int \cdots \int \mathrm{d}x_1 \ldots \mathrm{d}x_{N-1} \underbrace{\rho^{\text{free}}(x_0, x_1, \Delta_\tau)\, \rho^{\text{free}}(x_1, x_2, \Delta_\tau) \ldots \rho^{\text{free}}(x_{N-1}, x_N, \Delta_\tau)}_{\pi(x_1, \ldots, x_{N-1})}. \quad (3.45)$$

We focus for a moment on Monte Carlo moves where all positions except x_k are frozen, in particular x_{k-1} and x_{k+1}. Slightly generalizing the problem, we focus on a position x_k sandwiched in between fixed positions

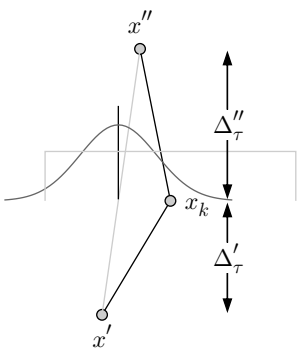

Fig. 3.12 Proposed and accepted moves in Alg. 3.4 (`naive-harmonic-path`). The position x_k is restrained by x' and x''.

Copyright © 2006. Oxford University Press, Incorporated. All rights reserved.

Krauth, Werner. Statistical Mechanics: Algorithms and Computations, Oxford University Press, Incorporated, 2006. ProQuest Ebook Central, http://ebookcentral.proquest.com/lib/tau/detail.action?docID=431021.
Created from tau on 2024-08-12 07:17:16.

x' and x'', with two intervals in τ, Δ'_τ and Δ''_τ (see Fig. 3.12). In the naive path-sampling algorithm, the move is drawn randomly between $-\delta$ and $+\delta$, around the current position x_k (see Fig. 3.12). The distribution of the accepted moves in Fig. 3.12 is given by

$$\pi^{\text{free}}(x_k|x', x'') \propto \rho^{\text{free}}(x', x_k, \Delta'_\tau)\, \rho^{\text{free}}(x_k, x'', \Delta''_\tau)\,,$$

where

$$\rho^{\text{free}}(x', x_k, \Delta'_\tau) \propto \exp\left[-\frac{(x'-x_k)^2}{2\Delta'_\tau}\right],$$
$$\rho^{\text{free}}(x_k, x'', \Delta''_\tau) \propto \exp\left[-\frac{(x_k-x'')^2}{2\Delta''_\tau}\right].$$

Expanding the squares and dropping all multiplicative terms independent of x_k, we find the following for the probability of x_k:

$$\underline{\pi^{\text{free}}(x_k|x', x'')} \propto \exp\left(-\frac{\cancel{x'^2} - 2x'x_k + x_k^2}{2\Delta'_\tau} - \frac{x_k^2 - 2x_k x'' + \cancel{x''^2}}{2\Delta''_\tau}\right)$$
$$\propto \underline{\exp\left[-\frac{(x_k - \langle x_k\rangle)^2}{2\sigma^2}\right]}, \quad (3.46)$$

where

$$\langle x_k\rangle = \frac{\Delta''_\tau x' + \Delta'_\tau x''}{\Delta'_\tau + \Delta''_\tau}$$

and

$$\sigma^2 = (1/\Delta''_\tau + 1/\Delta'_\tau)^{-1}.$$

The mismatch between the proposed moves and the accepted moves generates the rejections in the Metropolis algorithm. We could modify the naive path-sampling algorithm by choosing x_k from a Gaussian distribution with the appropriate parameters (taking $x' \equiv x_{k-1}$ (unless $k = 0$), $x'' \equiv x_{k+1}$, and $\Delta'_\tau = \Delta''_\tau = \beta/N$). In this way, no rejections would be generated.

The conditional probability in eqn (3.46) can be put to much better use than just to suppress a few rejected moves in a Markov-chain algorithm. In fact, $\pi^{\text{free}}(x_k|x', x'')$ gives the weight of all paths which, in Fig. 3.12, start at x', pass through x_k and end up at x''. We can sample this distribution to obtain x_1 (using $x' = x_0$ and $x'' = x_N$). Between the freshly sampled x_1 and x_N, we may then pick x_2, and thereafter x_3 between x_2 and x_N and, eventually, the whole path $\{x_1, \ldots, x_N\}$ (see Fig. 3.14 and Alg. 3.5 (`levy-free-path`)). A directly sampled path with $N = 50\,000$ is shown in Fig. 3.13; it can be generated in a split second, has no correlations with previous paths, and its construction has caused no rejections. In the limit $N \to \infty$, $x(\tau)$ is a differentiable continuous function of τ, which we shall further analyze in Section 3.5.

Direct path sampling—usually referred to as the Lévy construction—was introduced by Lévy (1940) as a stochastic interpolation between points x_0 and x_N. This generalizes interpolations using polynomials, trigonometric functions (see Subsection 3.5.1), splines, etc. The Lévy

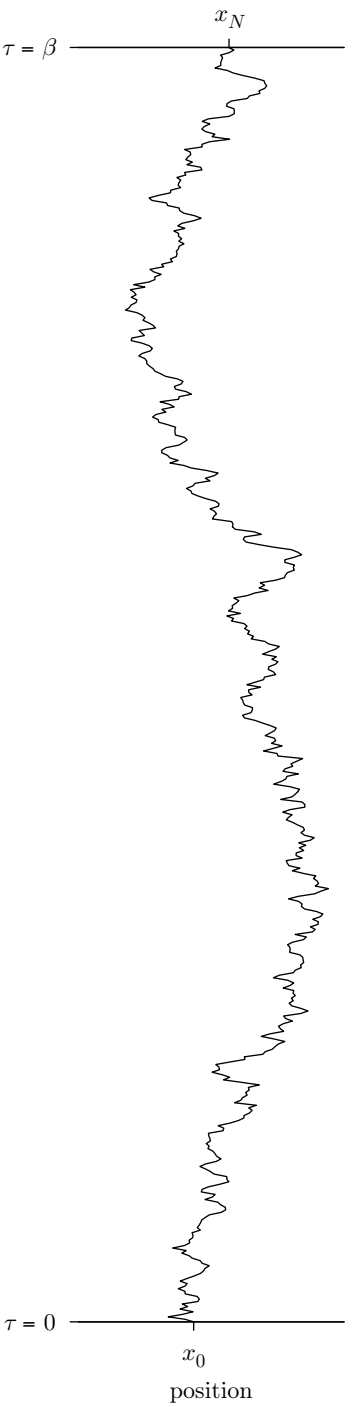

Fig. 3.13 A path contributing to $\rho^{\text{free}}(x_0, x_N, \beta)$ (from Alg. 3.5 (`levy-free-path`), with $N = 50\,000$).

Copyright © 2006. Oxford University Press, Incorporated. All rights reserved.

Krauth, Werner. Statistical Mechanics: Algorithms and Computations, Oxford University Press, Incorporated, 2006. ProQuest Ebook Central, http://ebookcentral.proquest.com/lib/tau/detail.action?docID=431021.
Created from tau on 2024-08-12 07:17:16.

construction satisfies a local construction principle: the path $x(\tau)$, in any interval $[\tau_1, \tau_2]$, is the stochastic interpolation of its end points $x(\tau_1)$ and $x(\tau_2)$, but the behavior of the path outside the interval plays no role.

The Lévy construction is related to the theory of stable distributions, also largely influenced by Lévy (see Subsection 1.4.4), essentially because Gaussians, which are stable distributions, are encountered at each step. The Lévy construction can be generalized to other stable distributions, but it then would not generate a continuous curve in the limit $\Delta_\tau \to 0$.

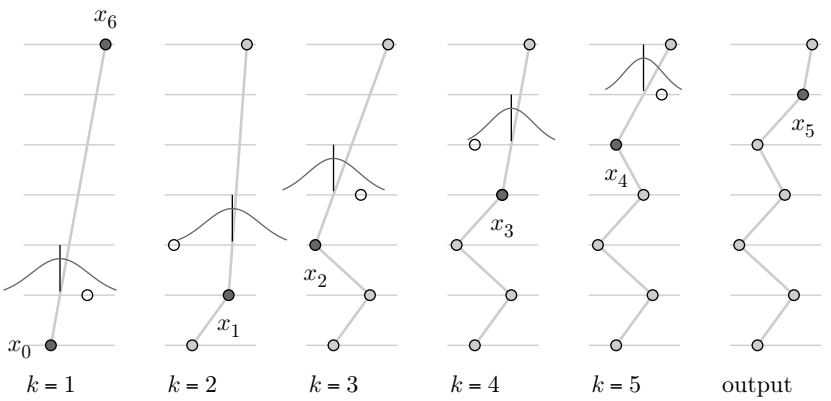

Fig. 3.14 Lévy construction of a free-particle path from x_0 to x_6 (see Alg. 3.5 (`levy-free-path`)).

procedure `levy-free-path`
input $\{x_0, x_N\}$
$\Delta_\tau \leftarrow \beta/N$
for $k = 1, \ldots, N-1$ **do**
$$\begin{cases} \Delta'_\tau \leftarrow (N-k)\Delta_\tau \\ \langle x_k \rangle \leftarrow (\Delta'_\tau x_{k-1} + \Delta_\tau x_N)/(\Delta_\tau + \Delta'_\tau) \\ \sigma^{-2} \leftarrow \Delta_\tau^{-1} + \Delta_\tau'^{-1} \\ x_k \leftarrow \langle x_k \rangle + \texttt{gauss}\,(\sigma) \end{cases}$$
output $\{x_0, \ldots, x_N\}$

Algorithm 3.5 `levy-free-path`. Sampling a path contributing to $\rho^{\text{free}}(x_0, x_N, \beta)$, using the Lévy construction (see Fig. 3.14).

We now consider the Lévy construction for a harmonic oscillator. The algorithm can be generalized to this case because the harmonic density matrix is a Gaussian (the exponential of a quadratic polynomial), and the convolution of two Gaussians is again a Gaussian:

$$\rho^{\text{h.o.}}(x', x'', \Delta'_\tau + \Delta''_\tau) = \int \mathrm{d}x_k \; \underbrace{\rho^{\text{h.o.}}(x', x_k, \Delta'_\tau)\, \rho^{\text{h.o.}}(x_k, x'', \Delta''_\tau)}_{\pi^{\text{h.o.}}(x_k | x', x'')}.$$

Copyright © 2006. Oxford University Press, Incorporated. All rights reserved.

Krauth, Werner. Statistical Mechanics: Algorithms and Computations, Oxford University Press, Incorporated, 2006. ProQuest Ebook Central, http://ebookcentral.proquest.com/lib/tau/detail.action?docID=431021.
Created from tau on 2024-08-12 07:17:16.

Because of the external potential, the mean value $\langle x_k \rangle$ no longer lies on the straight line between x' and x''. From the nondiagonal harmonic density matrix in eqn (3.37), and proceeding as in eqn (3.46), we find the following:

$$\pi^{\text{h.o.}}(x_k|x', x'') \propto \exp\left[-\frac{1}{2\sigma^2}\left(x_k - \langle x_k \rangle\right)^2\right],$$

with parameters

$$\begin{aligned}
\langle x_k \rangle &= \frac{\Upsilon_2}{\Upsilon_1}, \\
\sigma &= \Upsilon_1^{-1/2}, \\
\Upsilon_1 &= \coth\ \Delta'_\tau + \coth\ \Delta''_\tau, \\
\Upsilon_2 &= \frac{x'}{\sinh \Delta'_\tau} + \frac{x''}{\sinh \Delta''_\tau},
\end{aligned}$$

as already used in the analytic matrix squaring for the harmonic oscillator. We can thus directly sample paths contributing to the harmonic density matrix $\rho^{\text{h.o.}}(x_0, x_N, \beta)$ (see Alg. 3.6 (`levy-harmonic-path`)), and also paths contributing to $Z^{\text{h.o.}} = \int \mathrm{d}x_0\ \rho^{\text{h.o.}}(x_0, x_0, \beta)$, if we first sample x_0 from the Gaussian diagonal density matrix in eqn (3.38).

procedure `levy-harmonic-path`
input $\{x_0, x_N\}$
$\Delta_\tau \leftarrow \beta/N$
for $k = 1, \ldots, N-1$ **do**
$$\left\{\begin{array}{l}
\Upsilon_1 \leftarrow \coth \Delta_\tau + \coth\left[(N-k)\Delta_\tau\right] \\
\Upsilon_2 \leftarrow x_{k-1}/\sinh \Delta_\tau + x_N/\sinh\left[(N-k)\Delta_\tau\right] \\
\langle x_k \rangle \leftarrow \Upsilon_2/\Upsilon_1 \\
\sigma \leftarrow 1/\sqrt{\Upsilon_1} \\
x_k \leftarrow \langle x_k \rangle + \texttt{gauss}\,(\sigma)
\end{array}\right.$$
output $\{x_0, \ldots, x_N\}$

Algorithm 3.6 `levy-harmonic-path`. Sampling a path contributing to $\rho^{\text{h.o.}}(x_0, x_N, \beta)$, using the Lévy construction (see Fig. 3.15).

In Alg. 3.5 (`levy-free-path`), we were not obliged to sample the path in chronological order (first x_0, then x_1, then x_2, etc.). After fixing x_0 and x_N, we could have chosen to sample the midpoint $x_{N/2}$, then the midpoint between x_0 and $x_{N/2}$ and between $x_{N/2}$ and x_N, etc. (see Alg. 3.8 (`naive-box-path`) and Fig. 3.19 later). We finally note that free paths can also be directly sampled using Fourier-transformation methods (see Subsection 3.5.1).

3.3.3 Periodic boundary conditions, paths in a box

We now turn to free paths in a box, first with periodic boundary conditions, and then with hard walls. A path contributing to the density

Copyright © 2006. Oxford University Press, Incorporated. All rights reserved.

Krauth, Werner. Statistical Mechanics: Algorithms and Computations, Oxford University Press, Incorporated, 2006. ProQuest Ebook Central, http://ebookcentral.proquest.com/lib/tau/detail.action?docID=431021.
Created from tau on 2024-08-12 07:17:16.

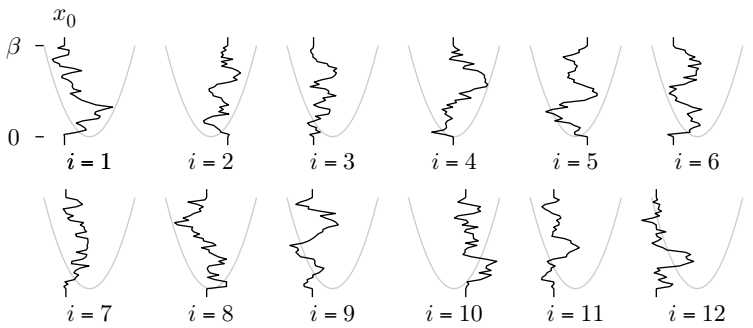

Fig. 3.15 Paths contributing to $Z^{\text{h.o.}} = \int \mathrm{d}x_0\, \rho^{\text{h.o.}}(x_0, x_0, \beta)$ (from Alg. 3.6 (`levy-harmonic-path`), with x_0 first sampled from eqn (3.38)).

matrix $\rho^{\text{per},L}(x, x', \beta)$ may wind around the box, that is, go from x to a periodic image $x' + wL$ rather than straight to x' (see Fig. 3.16, where the path $i = 1$ has zero winding number, the path $i = 2$ has a winding number $w = 1$, etc.).

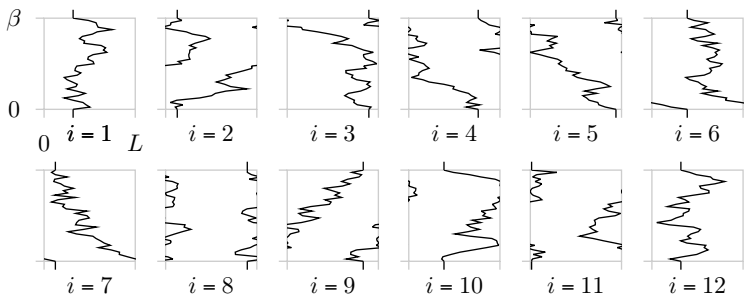

Fig. 3.16 Paths for a free particle in a periodic box (from Alg. 3.7 (`levy-periodic-path`) with $x_0 = \texttt{ran}\,(0, L)$).

The paths contributing to $\rho^{\text{per},L}(x, x', \beta)$ with a given winding number w are exactly the same as the paths contributing to $\rho^{\text{free}}(x, x' + wL, \beta)$. The total weight of all the paths contributing to $\rho^{\text{per},L}(x, x', \beta)$ is therefore $\sum_w \rho^{\text{free}}(x, x' + wL, \beta)$, and this is the expression for the density matrix in a periodic box that we already obtained in eqn (3.18), from the Poisson sum formula.

We can sample the paths contributing to the periodic density matrix by a two-step procedure: as each of the images $x_N + wL$ carries a statistical weight of $\rho^{\text{free}}(x_0, x_N + wL, \beta)$, we may first pick the winding number w by tower sampling (see Subsection 1.2.3). In the second step, the path between x_0 and $x_N + wL$ is filled in using the Lévy construction (see Alg. 3.7 (`levy-periodic-path`)).

The paths contributing to $\rho^{\text{box},[0,\,L]}(x, x', \beta)$ are the same as the free

Copyright © 2006. Oxford University Press, Incorporated. All rights reserved.

Krauth, Werner. Statistical Mechanics: Algorithms and Computations, Oxford University Press, Incorporated, 2006. ProQuest Ebook Central, http://ebookcentral.proquest.com/lib/tau/detail.action?docID=431021.
Created from tau on 2024-08-12 07:17:16.

procedure `levy-periodic-path`
input $\{x_0, x_N\}$
for $w' = \ldots, -1, 0, 1, \ldots$ **do**
$\{\ \pi_{w'} \leftarrow \rho^{\text{free}}(x_0, x_N + w'L, \beta)$
$w \leftarrow$ `tower sampling`$(\ldots, \pi_{-1}, \pi_0, \pi_1, \ldots)$
$\{x_1, \ldots, x_{N-1}\} \leftarrow$ `levy-free-path`$(x_0, x_N + wL, \beta)$
output $\{x_0, \ldots, x_N\}$

Algorithm 3.7 `levy-periodic-path`. Sampling a free path between x_0 and x_N in a box of length L with periodic boundary conditions.

paths, with the obvious restriction that they should not cross the boundaries. We have already shown that the density matrix of a free particle in a box satisfies

$$\rho^{\text{box},L}(x, x', \beta) = \sum_{w=-\infty}^{\infty} \left[\rho^{\text{free}}(x, x' + 2wL, \beta) - \rho^{\text{free}}(x, -x' + 2wL, \beta)\right]. \quad (3.47)$$

This is eqn (3.23) again. We shall now rederive it using a graphic method, rather than the Poisson sum formula of Subsection 3.1.3. Let us imagine boxes around an interval $[wL, (w+1)L]$, as in Fig. 3.17. For x and x' inside the interval $[0, L]$ (the original box), either the paths contributing to the free density matrix $\rho^{\text{free}}(x, x', \beta)$ never leave the box, or they reenter the box from the left or right boundary before connecting with x' at $\tau = \beta$:

$$\underbrace{\rho^{\text{free}}(x, x', \beta)}_{\substack{x \text{ and } x' \\ \text{in same box}}} = \underbrace{\rho^{\text{box}}(x, x', \beta)}_{\substack{\text{path does not} \\ \text{leave box}}} + \underbrace{\rho^{\text{right}}(x, x', \beta)}_{\substack{\text{path reenters} \\ \text{from right}}} + \underbrace{\rho^{\text{left}}(x, x', \beta)}_{\substack{\text{path reenters} \\ \text{from left}}} \quad (3.48)$$

(see Fig. 3.17).

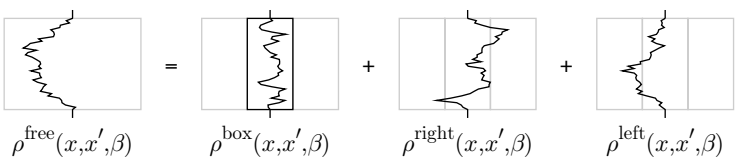

Fig. 3.17 Free density matrix as a sum of three classes of paths.

When x and x' are not in the same box, the path connects back to x' from either the right or the left border:

$$\underbrace{\rho^{\text{free}}(x, x', \beta)}_{\substack{x \text{ and } x' \\ \text{not in same box}}} = \underbrace{\rho^{\text{right}}(x, x', \beta)}_{\substack{\text{path enters box of } x' \\ \text{from right}}} + \underbrace{\rho^{\text{left}}(x, x', \beta)}_{\substack{\text{path enters box of } x' \\ \text{from left}}}.$$

Copyright © 2006. Oxford University Press, Incorporated. All rights reserved.

Krauth, Werner. Statistical Mechanics: Algorithms and Computations, Oxford University Press, Incorporated, 2006. ProQuest Ebook Central, http://ebookcentral.proquest.com/lib/tau/detail.action?docID=431021.
Created from tau on 2024-08-12 07:17:16.

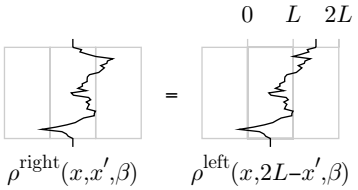

Fig. 3.18 A flip relation between left and right density matrices.

By flipping the final leg of a path, we can identify $\rho^{\rm right}(x,x',\beta)$ with $\rho^{\rm left}(x,2L-x',\beta)$ etc., (see Fig. 3.18):

$$\begin{aligned}\underline{\rho^{\rm right}(x,x',\beta)} &= \rho^{\rm left}(x,2L-x',\beta)\\ &= \rho^{\rm free}(x,2L-x',\beta) - \rho^{\rm right}(x,2L-x',\beta)\\ &= \rho^{\rm free}(x,2L-x',\beta) - \rho^{\rm left}(x,2L+x',\beta)\\ &= \underline{\rho^{\rm free}(x,2L-x',\beta) - \rho^{\rm free}(x,2L+x',\beta) + \rho^{\rm right}(x,2L+x',\beta)}.\end{aligned}$$

The density matrix $\rho^{\rm right}(x,2L+x',\beta)$ can itself be expressed through free density matrices around $4L$, so that we arrive at

$$\rho^{\rm right}(x,x',\beta) = \sum_{w=1}^{\infty}\left[\rho^{\rm free}(x,2wL-x',\beta) - \rho^{\rm free}(x,2wL+x',\beta)\right].$$

Analogously, we obtain

$$\begin{aligned}\rho^{\rm left}(x,x',\beta) &= \rho^{\rm free}(x,-x',\beta)\\ &+ \sum_{w=-1,-2,\ldots}\left[\rho^{\rm free}(x,2wL-x',\beta) - \rho^{\rm free}(x,2wL+x',\beta)\right].\end{aligned}$$

Entered into eqn (3.48), the last two equations yield the box density matrix.

We now sample the paths contributing to the density matrix in a box. Naively, we might start a Lévy construction, and abandon it after the first trespass over box boundaries. Within the naive approach, it is better to sample the path on large scales first, and then to work one's way to small scales (see Fig. 3.19 and Alg. 3.8 (`naive-box-path`)). Big moves, which carry a high risk of rejection, are made early. Bad paths are abandoned quickly.

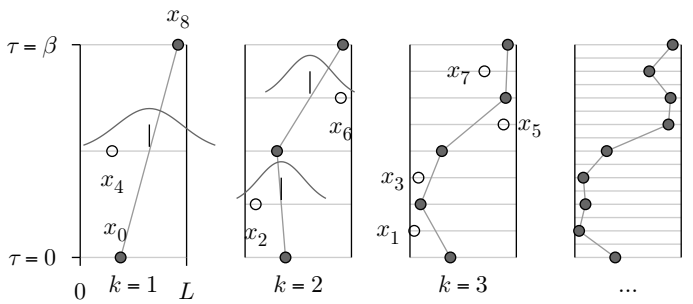

Fig. 3.19 Path construction in a box, on increasingly finer scales (in Alg. 3.8 (`naive-box-path`)).

Each path of the free density matrix that hits the boundary of the box contributes to the rejection rate of Alg. 3.8 (`naive-box-path`), given simply by

$$p_{\rm reject} = 1 - \frac{\rho^{{\rm box},[0,\,L]}(x,x',\beta)}{\rho^{\rm free}(x,x',\beta)}.$$

Copyright © 2006. Oxford University Press, Incorporated. All rights reserved.

Krauth, Werner. Statistical Mechanics: Algorithms and Computations, Oxford University Press, Incorporated, 2006. ProQuest Ebook Central, http://ebookcentral.proquest.com/lib/tau/detail.action?docID=431021.
Created from tau on 2024-08-12 07:17:16.

procedure `naive-box-path`
input $\{x_0, x_N\}$ (N is power of two: $N = 2^K$)
1 **for** $k = 1, \ldots, K$ **do**
  $\Delta_k \leftarrow 2^k$
  $\Delta_\tau \leftarrow \beta/\Delta_k$
    for $k' = 1, N/\Delta_k$ **do**
      $k \leftarrow k'\Delta_k$
      $k_\pm \leftarrow k \pm \Delta_k$
      $\langle x_{k'\Delta} \rangle \leftarrow \frac{1}{2}\left(x_{k_-} + x_{k_+}\right)$
      $x_k \leftarrow \langle x_{k_-} \rangle + \texttt{gauss}\left(\sqrt{2/\Delta_\tau}\right)$
      if ($x_k < 0$ or $x_k > L$) **goto** 1
output $\{x_0, \ldots, x_N\}$

Algorithm 3.8 `naive-box-path`. Sampling a path contributing to $\rho^{\mathrm{box},[0,\,L]}(x_0, x_N, \beta)$ from large scales down to small ones (see Fig. 3.19).

When $L \gg \sqrt{\beta}$, this rate is so close to one that the naive algorithm becomes impractical. We can then directly sample the positions x_k noting that, for example, the position x_4 in Fig. 3.19 is distributed as

$$\pi(x_4|x_0, x_8) = \underbrace{\rho^{\mathrm{box}}(x_0, x_4, \beta/2)\, \rho^{\mathrm{box}}(x_4, x_8, \beta/2)}_{\text{explicitly known, see eqn (3.47)}}.$$

This one-dimensional distribution can be sampled without rejections using the methods of Subsection 1.2.3, even though we must recompute it anew for each value of x_0 and x_8. We shall not pursue the discussion of this algorithm, but again see that elegant analytic solutions lead to superior sampling algorithms.

3.4 Pair density matrices

Using wave functions and energy eigenvalues on the one side, and density matrices on the other, we have so far studied single quantum particles in external potentials. It is time to move closer to the core of modern quantum statistical mechanics and to consider the many-body problem—mutually interacting quantum particles, described by many degrees of freedom. Path integral methods are important conceptual and computational tools to study these systems.

For concreteness, and also for consistency with other chapters, we illustrate the quantum many-body problem for a pair of three-dimensional hard spheres of radius σ. The density matrix for a pair of hard spheres can be computed with paths, but also in the old way, as in Section 3.1, with wave functions and eigenvalues. Both approaches have subtleties. The naive path integral for hard spheres is conceptually simple. It illustrates how the path integral approach maps a quantum system onto a classical system of interacting paths. However, it is computationally awkward, even for two spheres. On the other hand, the wave functions

Copyright © 2006. Oxford University Press, Incorporated. All rights reserved.

Krauth, Werner. Statistical Mechanics: Algorithms and Computations, Oxford University Press, Incorporated, 2006. ProQuest Ebook Central, http://ebookcentral.proquest.com/lib/tau/detail.action?docID=431021.
Created from tau on 2024-08-12 07:17:16.

and energy eigenvalues are not completely straightforward to obtain for a pair of hard spheres, but they then lead to a computationally fast, exact numerical solution for the pair density matrix. The two approaches come together in modern perfect action algorithms for the many-body problem, where analytical calculations are used to describe an N-body density matrix as a product of two-body terms, and where Monte Carlo calculations correct for the small error made in neglecting three-body and higher terms (see Subsection 3.4.3).

3.4.1 Two quantum hard spheres

We first consider noninteracting distinguishable particles, whose density matrix is the product of the individual density matrices because the wave function of pairs of noninteracting particles is the product of the single-particle wave functions. In the simplest terms, the density matrix is a sum of paths, and the paths for two or more distinguishable free particles in d dimensions can be put together from the individual uncorrelated d-dimensional paths, one for each particle. In the following, we shall imagine that these three-dimensional paths are generated by Algorithm `levy-free-path-3d`, which simply executes Alg. 3.5 (`levy-free-path`) three times: once for each Cartesian coordinate.

To sample paths contributing to the density matrix for a pair of hard spheres, we naively generate individual paths as if the particles were noninteracting. We reject them if particles approach to closer than twice the sphere radius σ, anywhere on their way from $\tau = 0$ to $\tau = \beta$:

$$\begin{aligned}\rho^{\text{pair}}(\{\mathbf{x}_0, \mathbf{x}_0'\}, \{\mathbf{x}_N, \mathbf{x}_N'\}, \beta) &= \left\{ \text{sum of paths} \right\} \\ &= \sum_{\text{paths } 1,2} \left\{ \begin{array}{c} \text{path 1:} \\ \mathbf{x}_0 \text{ to } \mathbf{x}_N \end{array} \right\} \left\{ \begin{array}{c} \text{path 2:} \\ \mathbf{x}_0' \text{ to } \mathbf{x}_N' \end{array} \right\} \left\{ \begin{array}{c} \text{nowhere} \\ \text{closer than } 2\sigma \end{array} \right\} \\ &= [1 - \underbrace{p^{\text{reject}}(\{\mathbf{x}_0, \mathbf{x}_0'\}, \{\mathbf{x}_N, \mathbf{x}_N'\}, \beta)}_{\text{rejection rate of Alg. 3.9}}] \rho^{\text{free}}(\mathbf{x}_0, \mathbf{x}_N, \beta)\, \rho^{\text{free}}(\mathbf{x}_0', \mathbf{x}_N', \beta)\end{aligned}$$

(see Fig. 3.20 and Alg. 3.9 (`naive-sphere-path`)). As discussed throughout this book, rejection rates of naive sampling algorithms often have a profound physical interpretation. The naive algorithm for a pair of quantum hard spheres is no exception to this rule.

```
     procedure naive-sphere-path
1    call levy-free-path-3d(x_0, x_N, β, N)
     call levy-free-path-3d(x'_0, x'_N, β, N)
     for k = 1, ..., N − 1 do
       { if (|x_k − x'_k| < 2σ) goto 1 (reject path—tabula rasa)
     output {{x_0, x'_0}, ..., {x_N, x'_N}}
```

Algorithm 3.9 `naive-sphere-path`. Sampling a path contributing to $\rho^{\text{pair}}(\{\mathbf{x}_0, \mathbf{x}_0'\}, \{\mathbf{x}_N, \mathbf{x}_N'\}, \beta)$ (see also Alg. 3.10).

Copyright © 2006. Oxford University Press, Incorporated. All rights reserved.

Krauth, Werner. Statistical Mechanics: Algorithms and Computations, Oxford University Press, Incorporated, 2006. ProQuest Ebook Central, http://ebookcentral.proquest.com/lib/tau/detail.action?docID=431021.
Created from tau on 2024-08-12 07:17:16.

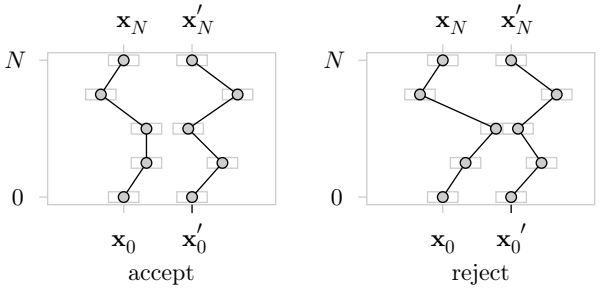

Fig. 3.20 Accepted and rejected configurations in Alg. 3.9 (`naive-sphere-path`) (schematic reduction from three dimensions).

When running Alg. 3.9 (`naive-sphere-path`), for example with $\mathbf{x}_0 = \mathbf{x}_N$ and $\mathbf{x}'_0 = \mathbf{x}'_N$, we notice a relatively high rejection rate (see Fig. 3.21). This can be handled for a single pair of hard spheres, but becomes prohibitive for the N-particle case. An analogous problem affected the direct sampling of classical hard spheres, in Subsection 2.2.1, and was essentially overcome by replacing the direct-sampling algorithm by a Markov-chain program. However, it is an even more serious issue that our approximation of the pair density matrix, the free density matrix multiplied by the acceptance rate of Alg. 3.9 (`naive-sphere-path`), strongly depends on the number of time slices. This means that we have to use very large values of N, that is, can describe two quantum hard spheres as a system of classical spheres connected by lines (as in Fig. 3.20), but only if there are many thousands of them.

As a first step towards better algorithms, we write the pair density matrix as a product of two density matrices, one for the relative motion and the other for the center-of-mass displacement. For a pair of free particles, we have

$$\begin{aligned}
&\rho^{\mathrm{free},m}(x_1,x'_1,\beta)\,\rho^{\mathrm{free},m}(x_2,x'_2,\beta) \\
&\qquad = \frac{m}{2\pi\beta}\exp\left[-\frac{m(x'_1-x_1)^2}{2\beta}-\frac{m(x'_2-x_2)^2}{2\beta}\right] \\
&= \sqrt{\frac{2m}{2\pi\beta}}\exp\left[-\frac{2m(X'-X)^2}{2\beta}\right]\sqrt{\frac{m/2}{2\pi\beta}}\exp\left[-\frac{m(\Delta'_x-\Delta_x)^2}{4\beta}\right] \\
&\qquad = \underbrace{\rho^{\mathrm{free},2m}(X,X',\beta)}_{\text{center of mass motion}}\ \underbrace{\rho^{\mathrm{free},\frac{1}{2}m}(\Delta_x,\Delta'_x,\beta)}_{\text{relative motion}}, \qquad (3.49)
\end{aligned}$$

where $X = \frac{1}{2}(x_1+x_2)$ and $X' = \frac{1}{2}(x'_1+x'_2)$ describe the center of mass and $\Delta_x = x_1 - x_2$ and $\Delta'_x = x'_1 - x'_2$ the relative distance. Clearly, interactions influence only the relative motion, and it suffices to generate single-particle paths corresponding to the relative coordinate describing a particle of reduced mass $\mu = m/2$ (or equivalently a particle of mass m at twice the inverse temperature 2β, see Alg. 3.10

The various terms in the second line of eqn (3.49) are rearranged as

$$\exp\left(-\frac{1}{2}A^2-\frac{1}{2}B^2\right) = \exp\left[-\frac{(A+B)^2}{4}-\frac{(A-B)^2}{4}\right]$$

Copyright © 2006. Oxford University Press, Incorporated. All rights reserved.

Krauth, Werner. Statistical Mechanics: Algorithms and Computations, Oxford University Press, Incorporated, 2006. ProQuest Ebook Central, http://ebookcentral.proquest.com/lib/tau/detail.action?docID=431021.
Created from tau on 2024-08-12 07:17:16.

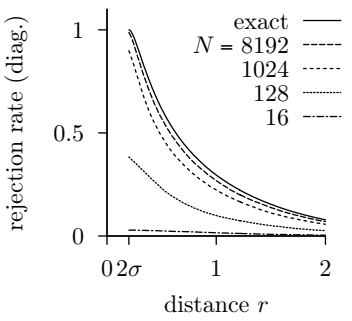

Fig. 3.21 Rejection rate of Alg. 3.9 (`naive-sphere-path`) (from Alg. 3.10, with $\beta = 4$, $2\sigma = 0.2$, $\Delta_{\mathbf{x},0} = \Delta_{\mathbf{x},N}$, and $r = |\Delta_{\mathbf{x},0}|$; for the exact solution see Subsection 3.4.2).

(`naive-sphere-path(patch)`)). (In the following, we set $m = 1$.) The new program runs twice as fast as Alg. 3.9 (`naive-sphere-path`), if we only compute the rejection rate. To recover the paths of the original algorithm, we must sample an independent free path for the center-of-mass variable $\mathbf{X}$ (a path for a particle of mass $2m$), and reconstruct the original variables as $\mathbf{x}_{1,2} = \mathbf{X} \pm \frac{1}{2}\Delta_{\mathbf{x}}$.

procedure `naive-sphere-path(patch)`
$\Delta_{\mathbf{x},0} \leftarrow \mathbf{x}'_0 - \mathbf{x}_0$
$\Delta_{\mathbf{x},N} \leftarrow \mathbf{x}'_N - \mathbf{x}_N$
call `levy-free-path-3d`$(\Delta_{\mathbf{x},0}, \Delta_{\mathbf{x},N}, 2\beta, N)$
for $k = 1, \ldots, N-1$ **do**
  if $(|\Delta_{\mathbf{x},k}| < 2\sigma)$ **then**
    output "reject"
    exit
output "accept"

Algorithm 3.10 `naive-sphere-path(patch)`. Computing the rejection rate of Alg. 3.9 from a single-particle simulation.

In conclusion, we have made first contact in this subsection with the path-integral Monte Carlo approach to interacting quantum systems. For concreteness, we considered the case of hard spheres, but other interaction potentials can be handled analogously, using the Trotter formula. We noted that the problem of two quantum hard spheres could be transformed into a problem involving a large number of interacting classical hard spheres. In Subsection 3.4.2, we shall find a more economical path-integral representation for quantum particles, which uses a much smaller number of time slices.

3.4.2 Perfect pair action

In Subsection 3.4.1, we tested a naive approach to the many-particle density matrix, one of the central objects of quantum statistical mechanics. The density matrix $\rho^{\text{pair}}(\{\mathbf{x}_0, \mathbf{x}'_0\}, \{\mathbf{x}_N, \mathbf{x}'_N\}, \beta)$ was computed by sending pairs of free paths from $\mathbf{x}_0$ to $\mathbf{x}_N$ and from $\mathbf{x}'_0$ to $\mathbf{x}'_N$. Any pair of paths that got too close was eliminated. All others contributed to the density matrix for a pair of hard spheres. Algorithm 3.9 (`naive-sphere-path`) can in principle be extended to more than two particles, and modified for arbitrary interactions. However, we must go to extremely large values of N in order for the discrete paths to really describe quantum hard spheres (see Fig. 3.21).

In Alg. 3.10 (`naive-sphere-path(patch)`), we separated the center-of-mass motion, which is unaffected by interactions, from the relative motion, which represents a single free particle of reduced mass $\mu = \frac{1}{2}$ that cannot penetrate into a region $r < 2\sigma$. Let us suppose, for a moment, that in addition the particle cannot escape to radii beyond a cutoff L (see Fig. 3.22; the cutoff will afterwards be pushed to infinity). This

Copyright © 2006. Oxford University Press, Incorporated. All rights reserved.

Krauth, Werner. Statistical Mechanics: Algorithms and Computations, Oxford University Press, Incorporated, 2006. ProQuest Ebook Central, http://ebookcentral.proquest.com/lib/tau/detail.action?docID=431021.
Created from tau on 2024-08-12 07:17:16.

three-dimensional free particle in a shell $r \in [2\sigma, L]$ has wave functions and eigenvalues just as the harmonic oscillator from the first pages of this chapter.

In the present subsection, we shall first compute these wave functions, and the energy eigenvalues, and then construct the hard-sphere pair density matrix much like we did in Alg. 3.2 (`harmonic-density`). We shall also see how to treat directly the $L = \infty$ limit. The calculation will need some basic mathematical concepts common to electrodynamics and quantum mechanics: the Laplace operator in spherical coordinates, the spherical Bessel functions, the spherical harmonics, and the Legendre polynomials. To simplify notation, we shall suppose that this particle of reduced mass $\mu = \frac{1}{2}$ is described by variables $\{x, y, z\}$, and replace them by the relative variables $\{\Delta_x, \Delta_y, \Delta_z\}$ in the final equations only.

In Subsection 3.4.3, we show how the analytical calculation of a pair density matrix can be integrated into a perfect-action Monte Carlo program, similar to those that have been much used in statistical mechanics and in field theory.

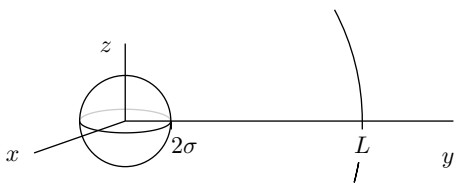

Fig. 3.22 Solving the Schrödinger equation for a free particle in a shell $r \in [2\sigma, L]$.

The three-dimensional Hamiltonian for a free particle of mass μ is

$$-\frac{\hbar^2}{2\mu}\underbrace{\left(\frac{\partial^2}{\partial x^2}+\frac{\partial^2}{\partial y^2}+\frac{\partial^2}{\partial z^2}\right)}_{\text{Laplace operator, } \nabla^2}\psi(x,y,z) = E\psi(x,y,z). \tag{3.50}$$

To satisfy the boundary conditions at $r = 2\sigma$ and $r = L$, we write the wave function $\psi(x, y, z) = \psi(r, \theta, \phi)$ and the Laplace operator ∇^2 in spherical coordinates:

$$\nabla^2\psi = \frac{1}{r}\frac{\partial^2}{\partial r^2}(r\psi) + \frac{1}{r^2\sin\theta}\frac{\partial}{\partial\theta}\left(\sin\theta\frac{\partial\psi}{\partial\theta}\right) + \frac{1}{r^2\sin^2\theta}\frac{\partial^2\psi}{\partial\phi^2}.$$

The wave function must vanish at $r = 2\sigma$ and for $r = L$. The differential equation (3.50) can be solved by the separation of variables:

$$\psi_{klm}(r,\theta,\phi) = Y_{lm}(\theta,\phi)R_{kl}(r),$$

where Y_{lm} are the spherical harmonic wave functions. For each value of l, the function $R_{kl}(r)$ must solve the radial Schrödinger equation

$$\left[-\frac{\hbar^2}{2\mu r^2}\frac{\partial}{\partial r}r^2\frac{\partial}{\partial r} + \frac{\hbar^2 l(l+1)}{2\mu r^2}\right]R_{kl}(r) = ER_{kl}(r).$$

Copyright © 2006. Oxford University Press, Incorporated. All rights reserved.

Krauth, Werner. Statistical Mechanics: Algorithms and Computations, Oxford University Press, Incorporated, 2006. ProQuest Ebook Central, http://ebookcentral.proquest.com/lib/tau/detail.action?docID=431021.
Created from tau on 2024-08-12 07:17:16.

The spherical Bessel functions $j_l(r)$ and $y_l(r)$ satisfy this differential equation. For small l, they are explicitly given by

$$j_0(r) = \frac{\sin r}{r}, \qquad y_0(r) = -\frac{\cos\ r}{r},$$
$$j_1(r) = \frac{\sin r}{r^2} - \frac{\cos\ r}{r}, \qquad y_1(r) = -\frac{\cos\ r}{r^2} - \frac{\sin r}{r}.$$

Spherical Bessel functions of higher order l are obtained by the recursion relation

$$f_{l+1}(r) = \frac{2l+1}{r} f_l(r) - f_{l-1}(r), \tag{3.51}$$

where f stands either for the functions $j_l(r)$ or for $y_l(r)$. We find, for example, that

$$j_2(r) = \left(\frac{3}{r^3} - \frac{1}{r}\right) \sin r - \frac{3}{r^2}\ \cos r,$$
$$y_2(r) = \left(-\frac{3}{r^3} + \frac{1}{r}\right) \cos r - \frac{3}{r^2}\ \sin r,$$

etc. (The above recursion relation is unstable numerically for large l and small r, but we only need it for $l \lesssim 3$.) For example, we can check that the function $j_0(r) = \sin r/r$, as all the other ones, is an eigenfunction of the radial Laplace operator with an eigenvalue equal to 1:

$$-\frac{1}{r^2}\frac{\partial}{\partial r} \underbrace{r^2 \frac{\partial}{\partial r}\left(\frac{\sin r}{r}\right)}_{r\cos r - \sin r} = -\frac{1}{r^2}\frac{\partial}{\partial r}\left(r\cos r - \sin r\right) = \overbrace{\left(\frac{\sin r}{r}\right)}^{j_0(r)}.$$

It follows that, analogously, all the functions $j_l(kr)$ and $y_l(kr)$ are solutions of the radial Schrödinger equation, with an eigenvalue

$$k^2 = 2\mu E_k \Leftrightarrow E_k = \frac{k^2}{2\mu}. \tag{3.52}$$

Besides satisfying the radial Schrödinger equation, the radial wave functions must vanish at $r = 2\sigma$ and $r = L$. The first condition, at $r = 2\sigma$, can be met by appropriately mixing $j_l(kr)$ and $y_l(kr)$, as follows:

$$R^{\delta}_{kl}(r) = \text{const} \cdot \left[j_l(kr)\cos\delta - y_l(kr)\sin\delta\right], \tag{3.53}$$

where the mixing angle δ satisfies

$$\delta = \arctan\frac{j_l(2k\sigma)}{y_l(2k\sigma)} \implies \cos\delta = \frac{y_l(2k\sigma)}{j_l(2k\sigma)}\sin\delta, \tag{3.54}$$

so that $R^{\delta}_{kl}(2\sigma) = 0$. The function $R^{\delta}_{kl}(r)$ vanishes at $r = L$ only for special values $\{k_0, k_1, \dots\}$. To find them, we can simply scan through the positive values of k using a small step size Δ_k. A change of sign between $R_{kl}(L)$ and $R_{(k+\Delta_k)l}(L)$ brackets a zero in the interval $[k, k+\Delta_k]$ (see Fig. 3.23 and Alg. 3.11 (`naive-rad-wavefunction`)). The three-

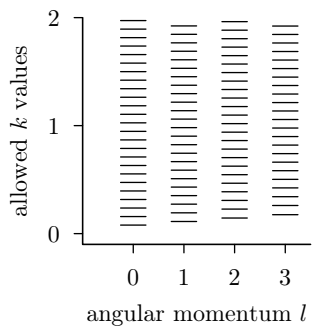

Fig. 3.23 Allowed k-values $\{k_0, k_1, \dots\}$ for small k (from Alg. 3.11 (`naive-rad-wavefunction`), with $2\sigma = 0.2$, and $L = 40$).

Copyright © 2006. Oxford University Press, Incorporated. All rights reserved.

Krauth, Werner. Statistical Mechanics: Algorithms and Computations, Oxford University Press, Incorporated, 2006. ProQuest Ebook Central, http://ebookcentral.proquest.com/lib/tau/detail.action?docID=431021.
Created from tau on 2024-08-12 07:17:16.

procedure `naive-rad-wavefunction`
input $\{r, \sigma, L\}$
$n \leftarrow 0$
for $k = 0, \Delta_k, \ldots$ **do**
  $\delta \leftarrow \arctan\left[j_l(2k\sigma)/y_l(2k\sigma)\right]$
  if $(R^{\delta}_{(k+\Delta_k)l}(L) R^{\delta}_{kl}(L) < 0)$ **then** (function $R^{\delta}_{kl}(r)$ from eqn (3.53))
    $k_n \leftarrow k$
    $\Upsilon \leftarrow 0$ (squared norm)
    for $r = 2\sigma, 2\sigma + \Delta_r, \ldots, L$ **do**
      $\Upsilon \leftarrow \Upsilon + \Delta_r r^2 [R^{\delta}_{k_n l}(r)]^2$
    output $\{k_n, \{R_{k_n l}(2\sigma)/\sqrt{\Upsilon}, \ldots, R_{k_n l}(L)/\sqrt{\Upsilon}\}\}$
    $n \leftarrow n + 1$

Algorithm 3.11 `naive-rad-wavefunction`. Computing normalized radial wave functions that vanish at $r = 2\sigma$ and at $r = L$.

dimensional wave functions must be normalized, i.e. must satisfy the relation

$$\int \mathrm{d}^3\mathbf{x}\ |\psi_{klm}(\mathbf{x})|^2 = \underbrace{\int \mathrm{d}\Omega\ Y_{lm}(\theta,\phi) Y^*_{lm}(\theta,\phi)}_{=1} \underbrace{\int_{2\sigma}^{L} \mathrm{d}r\ r^2 R^2_{kl}(r)}_{\text{must be } 1} = 1.$$

The normalization condition on the radial wave functions is taken into account in Alg. 3.11 (`naive-rad-wavefunction`).

With the normalized radial wave functions $R^{\delta}_{k_n l}(r)$, which vanish at $r = 2\sigma$ and $r = L$, and which have eigenvalues as shown in eqn (3.52), we have all that it takes to compute the density matrix

$$\rho^{\mathrm{rel}}(\Delta_{\mathbf{x}_0}, \Delta_{\mathbf{x}_N}, \beta) = \sum_{l=0}^{\infty} \underbrace{\sum_{m=-l}^{l} Y^*_{lm}(\theta_0,\phi_0) Y_{lm}(\theta_N,\phi_N)}_{\frac{2l+1}{4\pi} P_l(\cos\gamma)} \times \sum_{n=0,1,\ldots} \exp\left(-\beta \frac{k_n^2}{2\mu}\right) R_{k_n l}(r_0) R_{k_n l}(r_N). \quad (3.55)$$

Here, the relative coordinates are written in polar coordinates $\Delta_{\mathbf{x}_0} = \{r_0, \theta_0, \phi_0\}$ and $\Delta_{\mathbf{x}_N} = \{r_N, \theta_N, \phi_N\}$. Furthermore, we have expressed in eqn (3.55) the sum over products of the spherical harmonics through the Legendre polynomials $P_l(\cos\gamma)$, using a standard relation that is familiar from classical electrodynamics and quantum mechanics. The argument of the Legendre polynomial involves the opening angle γ between the vectors $\Delta_{\mathbf{x}_0}$ and $\Delta_{\mathbf{x}_N}$, defined by the scalar product $(\Delta_{\mathbf{x}_0} \cdot \Delta_{\mathbf{x}_N}) = r_0 r_N \cos\gamma$.

The Legendre polynomials P_l could be computed easily, but for concreteness, we consider here only the diagonal density matrix, where $\Delta_{\mathbf{x}_0} = \Delta_{\mathbf{x}_N}$ (so that $\gamma = 0$). In this case, the Legendre polynomials

Copyright © 2006. Oxford University Press, Incorporated. All rights reserved.

Krauth, Werner. Statistical Mechanics: Algorithms and Computations, Oxford University Press, Incorporated, 2006. ProQuest Ebook Central, http://ebookcentral.proquest.com/lib/tau/detail.action?docID=431021.
Created from tau on 2024-08-12 07:17:16.

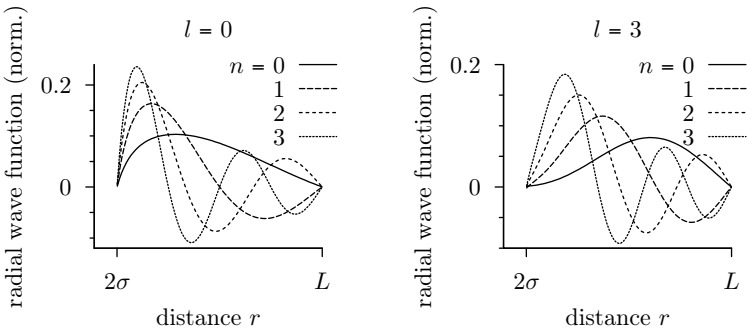

Fig. 3.24 Normalized radial wave functions $R^{\delta}_{k_n l}$ (from Alg. 3.11 (`naive-rad-wavefunction`), with $2\sigma = 1$ and $L = 10$).

are all equal to 1 ($P_l(1) = 1$), so that we do not have to provide a subroutine.

The relative-motion density matrix in eqn (3.55) is related to the density matrix for a pair of hard spheres as follows:

$$\rho^{\text{pair}}(\{\mathbf{x}_0, \mathbf{x}'_0\}, \{\mathbf{x}_N, \mathbf{x}'_N\}, \beta) = \underbrace{\left[\frac{\rho^{\text{pair}}(\{\mathbf{x}_0, \mathbf{x}'_0\}, \{\mathbf{x}_N, \mathbf{x}'_N\}, \beta)}{\rho^{\text{free}}(\mathbf{x}_0, \mathbf{x}_N, \beta)\, \rho^{\text{free}}(\mathbf{x}'_0, \mathbf{x}'_N, \beta)}\right]}_{\text{depends on } \Delta_{\mathbf{x}} \text{ and } \Delta'_{\mathbf{x}}, \text{ only}} \times \rho^{\text{free}}(\mathbf{x}_0, \mathbf{x}_N, \beta)\, \rho^{\text{free}}(\mathbf{x}'_0, \mathbf{x}'_N, \beta)\,, \quad (3.56)$$

where it is crucial that the piece in square brackets can be written as a product of center-of-mass density matrices and of relative-motion density matrices. The latter cancel, and we find

$$\left[\frac{\rho^{\text{pair}}(\{\mathbf{x}_0, \mathbf{x}'_0\}, \{\mathbf{x}_N, \mathbf{x}'_N\}, \beta)}{\rho^{\text{free}}(\mathbf{x}_0, \mathbf{x}_N, \beta)\, \rho^{\text{free}}(\mathbf{x}'_0, \mathbf{x}'_N, \beta)}\right] = \left[\frac{\rho^{\text{rel},\mu=\frac{1}{2}}(\Delta_{\mathbf{x}_0}, \Delta_{\mathbf{x}_N}, \beta)}{\rho^{\text{free},\mu=\frac{1}{2}}(\Delta_{\mathbf{x}_0}, \Delta_{\mathbf{x}_N}, \beta)}\right].$$

To obtain the virtually exact results shown in Fig. 3.21, it suffices to compute, for $l = \{0, \ldots, 3\}$, the first 25 wave numbers $\{k_0, \ldots, k_{24}\}$ for which the wave functions satisfy the boundary conditions (the first four of them are shown in Fig. 3.24, for $l = 0$ and $l = 3$) (see Table 3.2; the diagonal free density matrix is $\left(1/\sqrt{4\pi\beta}\right)^3 = 0.0028$).

The density matrix for the relative motion can be computed directly in the limit $L \to \infty$ because the functions $j_l(r)$ and $y_l(r)$ behave as $\pm \sin(r)/r$ or $\pm \cos(r)/r$ for large r. (This follows from the recursion relation in eqn (3.51).) The normalizing integral becomes

$$\Upsilon = \int_a^L \mathrm{d}r\; r^2 [j_l(kr)]^2 \xrightarrow{L\to\infty} \frac{1}{k^2} \int_a^L \mathrm{d}r\; \sin^2(kr) = \frac{L}{2k^2}.$$

Table 3.2 Relative density matrix $\rho^{\text{rel}}(\Delta_{\mathbf{x},0}, \Delta_{\mathbf{x},N}, \beta)$, and rejection rate of Alg. 3.9 (`naive-sphere-path`) (from Alg. 3.11 (`naive-rad-wavefunction`) and eqn (3.55), with $\beta = 4$, $2\sigma = 0.2$, $\Delta_{\mathbf{x},0} = \Delta_{\mathbf{x},N}$ ($r = |\Delta_{\mathbf{x},0}|$, compare with Fig. 3.21)).

r	ρ^{rel}	Rejection rate
0.2	0.00000	1.00
0.4	0.00074	0.74
0.6	0.00134	0.52
0.8	0.00172	0.39
1.0	0.00198	0.30

Copyright © 2006. Oxford University Press, Incorporated. All rights reserved.

Krauth, Werner. Statistical Mechanics: Algorithms and Computations, Oxford University Press, Incorporated, 2006. ProQuest Ebook Central, http://ebookcentral.proquest.com/lib/tau/detail.action?docID=431021.
Created from tau on 2024-08-12 07:17:16.

The asymptotic behavior of the spherical Bessel functions also fixes the separation between subsequent k-values to $\Delta_k = \pi/L$. (Under this condition, subsequent functions satisfy $\sin(kL) = 0$ and $\sin[(k+\Delta_k)L] = 0$, etc., explaining why there are about 25 states in an interval of length $\pi 25/40 \simeq 2.0$, in Fig. 3.23). The sum over discrete eigenvalues n can then be replaced by an integral:

$$\sum_k \cdots = \frac{1}{\Delta_k} \sum_k \Delta_k \cdots \simeq \frac{1}{\Delta_k} \int \mathrm{d}k \ \ldots ,$$

and we arrive at the following pair density matrix in the limit $L \to \infty$:

$$\rho^{\mathrm{rel}}(\mathbf{x}, \mathbf{x}', \beta) = \sum_{l=0}^{\infty} P_l(\cos\gamma) \frac{2l+1}{4\pi} \times \int_{k=0}^{\infty} \mathrm{d}k \ \exp\left(-\beta \frac{k^2}{2\mu}\right) \hat{R}^{\delta}_{kl}(r) \hat{R}^{\delta}_{kl}(r'). \quad (3.57)$$

In this equation, we have incorporated the constant stemming from the normalization and from the level spacing Δ_k into the radial wave function:

$$\hat{R}^{\delta}(r) = \sqrt{\frac{2}{\pi} k} \left[j_l(kr) \cos\delta - y_l(kr) \sin\delta \right].$$

The integrals in eqn (3.57) are done numerically (except for $l = 0$). The mixing angles $\delta(k, \sigma)$ ensure that $\tilde{R}^{\delta}_{kl}(2\sigma) = 0$ for all k (see eqn (3.54)).

In conclusion, we have computed in this subsection the exact statistical weight for all continuous hard-sphere paths going through a discretized set of position $\{\mathbf{x}_0, \ldots, \mathbf{x}_N\}$ and $\{\mathbf{x}'_0, \ldots, \mathbf{x}'_N\}$ (see Fig. 3.25). For clarity, let us collect variables on one slice k into a single symbol $\mathcal{X}_k \equiv \{\mathbf{x}_k, \mathbf{x}'_k\}$. The weight of a discretized path, the exponential of the action $\mathcal{S}$, was determined as

$$\left\{ \begin{matrix} \text{weight} \\ \text{of path} \end{matrix} \right\} \propto \exp\left[-\mathcal{S}(\{\mathcal{X}_0, \ldots, \mathcal{X}_N\}, \Delta_\tau)\right] = \rho^{\mathrm{pair}}(\mathcal{X}_0, \mathcal{X}_1, \Delta_\tau) \times \cdots \times \rho^{\mathrm{pair}}(\mathcal{X}_{N-1}, \mathcal{X}_N, \Delta_\tau). \quad (3.58)$$

Previously, the naive action $\mathcal{S}$ was either zero or infinite, and it described a pair of hard spheres badly, unless Δ_τ was very small. In contrast, the weight of a path, in eqn (3.58), is assembled from the pair density matrices. It describes a pair of hard spheres exactly, at any Δ_τ, and it corresponds to the "perfect pair action" $\mathcal{S}(\{\mathcal{X}_0, \ldots, \mathcal{X}_N\}, \Delta_\tau)$.

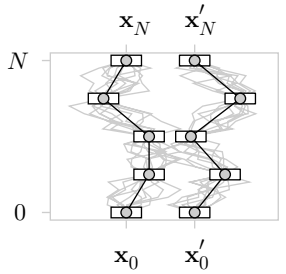

Fig. 3.25 A pair of discretized paths, representing continuous paths of hard spheres.

3.4.3 Many-particle density matrix

The pair density matrix from Subsection 3.4.2 links up with the full quantum N-body problem (for concreteness, we continue with the example of quantum hard spheres). It is easily generalized from two to N

Copyright © 2006. Oxford University Press, Incorporated. All rights reserved.

Krauth, Werner. Statistical Mechanics: Algorithms and Computations, Oxford University Press, Incorporated, 2006. ProQuest Ebook Central, http://ebookcentral.proquest.com/lib/tau/detail.action?docID=431021.
Created from tau on 2024-08-12 07:17:16.

particles:

$$\rho^{N\text{-part}}(\{\mathbf{x}_1,\ldots,\mathbf{x}_N\},\{\mathbf{x}'_1,\ldots,\mathbf{x}'_N\},\Delta_\tau) \simeq \left\{\prod_{k=1}^{N}\rho^{\text{free}}(\mathbf{x}_k,\mathbf{x}'_k,\Delta_\tau)\right\}\prod_{k<l}\underbrace{\frac{\rho^{\text{pair}}(\{\mathbf{x}_k,\mathbf{x}_l\},\{\mathbf{x}'_k,\mathbf{x}'_l\},\Delta_\tau)}{\rho^{\text{free}}(\mathbf{x}_k,\mathbf{x}'_k,\Delta_\tau)\,\rho^{\text{free}}(\mathbf{x}_l,\mathbf{x}'_l,\Delta_\tau)}}_{\text{prob. that paths } k \text{ and } l \text{ do not collide}}. \quad (3.59)$$

For two particles, this is the same as eqn (3.56), and it is exact. For N particles, eqn (3.59) remains correct under the condition that we can treat the collision probabilities for any pair of particles as independent of those for other pairs. This condition was already discussed in the context of the virial expansion for classical hard spheres (see Subsection 2.2.2). It is justified at low density or at high temperature. In the first case (low density) paths rarely collide, so that the paths interfere very little. In the second case (Δ_τ corresponding to high temperature), the path of particle k does not move away far from the position $\mathbf{x}_k \simeq \mathbf{x}'_k$, and the interference of paths is again limited. Because of the relation $\Delta_\tau = \beta/N$, we can always find an appropriate value of N for which the N-density matrix in eqn (3.59) is essentially exact. The representation of the density matrix in eqn (3.59) combines elements of a high-temperature expansion and of a low-density expansion. It is sometimes called a Wigner–Kirkwood expansion.

In all practical cases, the values of N that must be used are much smaller than the number of time slices needed in the naive approach of Subsection 3.4.1 (see Pollock and Ceperley (1984), Krauth (1996)).

3.5 Geometry of paths

Quantum statistical mechanics can be formulated in terms of random paths in space and imaginary time. This is the path-integral approach that we started to discuss in Sections 3.3 and 3.4, and for which we have barely scratched the surface. Rather than continue with quantum statistics as it is shaped by path integrals, we analyze in this section the shapes of the paths themselves. This will lead us to new sampling algorithms using Fourier transformation methods. The geometry of paths also provides an example of the profound connections between classical statistical mechanics and quantum physics, because random paths do not appear in quantum physics alone. They can describe cracks in homogeneous media (such as a wall), interfaces between different media (such as between air and oil in a suspension) or else between different phases of the same medium (such as the regions of a magnet with different magnetizations). These interfaces are often very rough. They then resemble the paths of quantum physics, and can be described by very similar methods. This will be the subject of Subsection 3.5.3.

Copyright © 2006. Oxford University Press, Incorporated. All rights reserved.

Krauth, Werner. Statistical Mechanics: Algorithms and Computations, Oxford University Press, Incorporated, 2006. ProQuest Ebook Central, http://ebookcentral.proquest.com/lib/tau/detail.action?docID=431021.
Created from tau on 2024-08-12 07:17:16.

3.5.1 Paths in Fourier space

In the following, we describe paths by use of Fourier variables, the coefficients of trigonometric functions. For computer implementation, we remain primarily interested in discrete paths $\{x_0, \ldots, x_N\}$, but we treat continuous paths first because they are mathematically simpler. As a further simplification, we consider here paths which start at zero and return back to zero ($x(0) = x(\beta) = 0$). Other cases will be considered in Subsection 3.5.3.

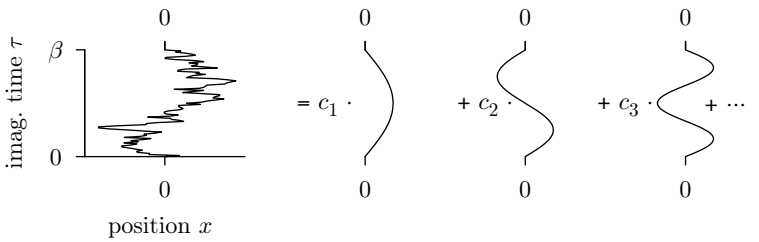

Fig. 3.26 Representation of a continuous path $x(\tau)$ as an infinite sum over Fourier modes.

Any path $x(\tau)$ with $x(0) = x(\beta) = 0$ can be decomposed into an infinite set of sine functions:

$$x(\tau) = \sum_{n=1}^{\infty} c_n \sin\left(n\pi\frac{\tau}{\beta}\right) \quad \tau \in [0, \beta] \tag{3.60}$$

(see Fig. 3.26). The sine functions in eqn (3.60) are analogous to the wave functions $\psi_n^{\text{box}}(x)$, the solutions of the Schrödinger equation in a box with walls (see Subsection 3.1.3). Now, however, we consider a path, a function of τ from 0 to β, rather than a wave function, extending in x, from 0 to L. The difference between pure sine functions and the combined series of sines and cosines mirrors the one between wave functions with hard walls and with periodic boundary conditions.

Each path $x(\tau)$ contributing to the density matrix $\rho^{\text{free}}(0, 0, \beta)$ is described by Fourier coefficients $\{c_0, c_1, \ldots\}$. We first determine these coefficients for a given path and then express the weight of each path, and the density matrix, directly in Fourier space. The coefficients are obtained from the orthonormality relation of Fourier modes:

$$\int_0^\beta \mathrm{d}\tau \quad \underbrace{\sin\left(n\pi\frac{\tau}{\beta}\right)\sin\left(l\pi\frac{\tau}{\beta}\right)}_{\frac{1}{2}\{\cos[(n-l)\pi\tau/\beta]-\cos[(n+l)\pi\tau/\beta]\}} = \frac{\beta}{2}\delta_{nl}. \tag{3.61}$$

We can project out the coefficient c_l of mode l by multiplying the Fourier representation of a path, in eqn (3.60), on both sides by $\sin(l\pi\tau/\beta)$ and

Copyright © 2006. Oxford University Press, Incorporated. All rights reserved.

Krauth, Werner. Statistical Mechanics: Algorithms and Computations, Oxford University Press, Incorporated, 2006. ProQuest Ebook Central, http://ebookcentral.proquest.com/lib/tau/detail.action?docID=431021.
Created from tau on 2024-08-12 07:17:16.

integrating over τ from 0 to β,

$$\underline{\frac{2}{\beta}\int_0^\beta \mathrm{d}\tau\ \sin\left(l\pi\frac{\tau}{\beta}\right)x(\tau)} = \frac{2}{\beta}\int_0^\beta \mathrm{d}\tau\ \sin\left(l\pi\frac{\tau}{\beta}\right)\sum_{n=1}^{\infty} c_n \sin\left(n\pi\frac{\tau}{\beta}\right)$$
$$= \frac{2}{\beta}\sum_{n=1}^{\infty} c_n \underbrace{\int_0^\beta \mathrm{d}\tau\ \sin\left(l\pi\frac{\tau}{\beta}\right)\sin\left(n\pi\frac{\tau}{\beta}\right)}_{(\beta/2)\delta_{ln};\ \text{see eqn (3.61)}} = \underline{c_l}. \quad (3.62)$$

We can thus determine the Fourier coefficients $\{c_1, c_2, \dots\}$ for a given function $x(\tau)$, whereas eqn (3.60) allowed us to compute the function $x(\tau)$ for given Fourier coefficients.

We now express the statistical weight of the path $\{x_0, \dots, x_N\}$ directly in Fourier variables. With $\Delta_\tau = \beta/N$, we find

$$\left\{\begin{matrix}\text{weight}\\ \text{of path}\end{matrix}\right\} = \exp\left[-\mathcal{S}(\{x_0, \dots, x_N\})\right]$$
$$= \rho^{\text{free}}(x_0, x_1, \Delta_\tau)\,\rho^{\text{free}}(x_1, x_2, \Delta_\tau) \times \cdots \times \rho^{\text{free}}(x_{N-1}, x_N, \Delta_\tau)\,.$$

In the small-Δ_τ limit, each term in the action can be written as

$$\frac{1}{2}\frac{(x-x')^2}{\Delta_\tau} = \frac{1}{2}\Delta_\tau\frac{(x-x')^2}{\Delta_\tau^2} \to \frac{1}{2}\mathrm{d}\tau\left[\frac{\partial x(\tau)}{\partial\tau}\right]^2 \quad (3.63)$$

and summing over all terms, in the limit $\Delta_\tau \to 0$, corresponds to an integration from 0 to β. In this limit, the action becomes

$$\mathcal{S} = \frac{1}{2}\int_0^\beta \mathrm{d}\tau\ \left[\frac{\partial x(\tau)}{\partial\tau}\right]^2. \quad (3.64)$$

We use this formula to express the action in Fourier space, using the Fourier representation of the path given in eqn (3.60). The derivative with respect to τ gives

$$\frac{\partial}{\partial\tau}x(\tau) = \sum_{n=1}^{\infty} c_n \frac{n\pi}{\beta}\cos\left(n\pi\frac{\tau}{\beta}\right).$$

The action in eqn (3.64) leads to a double sum of terms $\propto c_n c_m$ that is generated by the squared derivative. However, the nondiagonal terms again vanish. We arrive at

$$\frac{1}{2}\int_0^\beta \mathrm{d}\tau\left(\frac{\partial x}{\partial\tau}\right)^2 = \frac{1}{2}\sum_{n=1}^{\infty} c_n^2\frac{n^2\pi^2}{\beta^2}\underbrace{\int_0^\beta \mathrm{d}\tau\ \cos^2\left(n\pi\frac{\tau}{\beta}\right)}_{\beta/2} = \frac{1}{\beta}\sum_{n=1}^{\infty}\frac{c_n^2 n^2\pi^2}{4}.$$

We should note that the derivative of $x(\tau)$ and the above exchange of differentiation and integration supposes that the function $x(\tau)$ is sufficiently smooth. We simply assume that the above operations are well defined. The statistical weight of a path is then given by

$$\left\{\begin{matrix}\text{weight of}\\ \text{path}\end{matrix}\right\} \propto \exp\left(-\frac{1}{\beta}\sum_{n=1}^{\infty} c_n^2\frac{n^2\pi^2}{4}\right),$$

Copyright © 2006. Oxford University Press, Incorporated. All rights reserved.

Krauth, Werner. Statistical Mechanics: Algorithms and Computations, Oxford University Press, Incorporated, 2006. ProQuest Ebook Central, http://ebookcentral.proquest.com/lib/tau/detail.action?docID=431021.
Created from tau on 2024-08-12 07:17:16.

and the density matrix, written in terms of Fourier variables, is an infinite product of integrals:

$$\rho^{\text{free}}(0,0,\beta) \propto \prod_{n=1}^{\infty} \left[\int_{-\infty}^{\infty} \frac{\mathrm{d}c_n n\pi}{\sqrt{4\pi\beta}} \exp\left(-\frac{1}{\beta} \sum_{n=1}^{\infty} c_n^2 \frac{n^2\pi^2}{4} \right) \right].$$

The Fourier transform of a continuous path is operationally quite simple but, as mentioned, hides mathematical subtleties. These difficulties are absent for the Fourier transformation of discrete paths $\{x_0, \ldots, x_N\}$, a subject we now turn to.

A discrete function $\{x_0, \ldots, x_N\}$ can be represented by a finite number N of Fourier modes:

$$x_k = \sum_{n=1}^{N-1} c_n \sin\left(n\pi \frac{k}{N} \right) \quad k = 0, \ldots, N \tag{3.65}$$

(see Fig. 3.27). Remarkably, the discrete sine functions remain mutually orthogonal if we simply replace the integral over τ in the orthogonality condition in eqn (3.61) by the sum over a discrete index k:

In the following, k and j are discretized τ indices, and n and l describe Fourier modes.

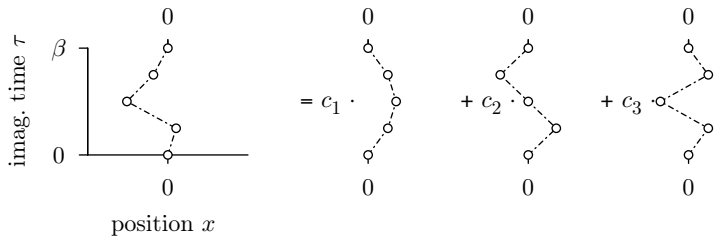

Fig. 3.27 Representation of a discrete path $\{x_0, \ldots, x_4\}$ as a finite sum over Fourier modes.

$$\sum_{k=1}^{N-1} \underbrace{\sin\left(n\pi \frac{k}{N} \right) \sin\left(l\pi \frac{k}{N} \right)}_{\frac{1}{2}\{\cos[(n-l)\pi k/N] - \cos[(n+l)\pi k/N]\}} = \frac{N}{2}\delta_{nl}. \tag{3.66}$$

Equation (3.66) can be checked in exponential notation ($\cos x = \mathrm{Re}(\mathrm{e}^{\mathrm{i}x})$) by summing the geometric series for noninteger M/N:

$$\sum_{k=0}^{N-1} \cos M\pi \frac{k}{N} = \mathrm{Re} \sum_{k=0}^{N-1} \exp\left(\mathrm{i}\pi \frac{M}{N} \right)^k = \mathrm{Re}\left[\frac{1 - \mathrm{e}^{\mathrm{i}M\pi}}{1 - \exp\left(\mathrm{i}\frac{M}{N}\pi \right)} \right]. \tag{3.67}$$

In eqn (3.66), $(n - l)$ and $(n + l)$ are either both even or odd. In the first case, the sum in eqn (3.67) is zero. In the second, the two sums are easily seen to be equal. They thus cancel.

Copyright © 2006. Oxford University Press, Incorporated. All rights reserved.

Krauth, Werner. Statistical Mechanics: Algorithms and Computations, Oxford University Press, Incorporated, 2006. ProQuest Ebook Central, http://ebookcentral.proquest.com/lib/tau/detail.action?docID=431021.
Created from tau on 2024-08-12 07:17:16.

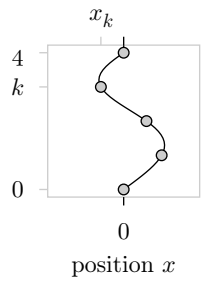

Fig. 3.28 Example path $\{x_0, \ldots, x_N\}$ of eqn (3.69). The trigonometric polynomial defined in eqn (3.70) passes through all the points.

Again multiplying the discrete function x_k of eqn (3.65) on both sides by $\sin(l\pi k/N)$ and summing over l, we find

$$\underline{\frac{2}{N}\sum_{k=1}^{N-1}\sin\left(l\pi\frac{k}{N}\right)x_k} = \frac{2}{N}\sum_{k=1}^{N-1}\sin\left(l\pi\frac{k}{N}\right)\sum_{n=1}^{N-1}c_n\sin\left(n\pi\frac{k}{N}\right)$$
$$= \frac{2}{N}\sum_{n=1}^{N-1}c_n\underbrace{\sum_{k=1}^{N-1}\sin\left(l\pi\frac{k}{N}\right)\sin\left(n\pi\frac{k}{N}\right)}_{\frac{1}{2}N\delta_{ln},\ \text{see eqn (3.66)}} = \underline{c_l}, \quad (3.68)$$

in analogy with eqn (3.62). The $N-1$ Fourier coefficients $\{c_1, \ldots, c_{N-1}\}$ define a trigonometric interpolating polynomial $x(\tau)$ which passes exactly through the points $\{x_0, \ldots, x_N\}$ and which contains the same information as the Fourier coefficients. To illustrate this point, let us consider an example path for $N = 4$ described by the two sets of variables:

$$\overbrace{\begin{bmatrix} x_0 \\ x_1 \\ x_2 \\ x_3 \\ x_4 \end{bmatrix} = \begin{bmatrix} 0.0 \\ 0.25 \\ 0.15 \\ -0.15 \\ 0.0 \end{bmatrix}}^{\text{real-space variables (in Fig. 3.28)}} \equiv \overbrace{\begin{bmatrix} c_0 \\ c_1 \\ c_2 \\ c_3 \\ c_4 \end{bmatrix} = \begin{bmatrix} 0.0 \\ 0.1104 \\ 0.2 \\ -0.039 \\ 0.0 \end{bmatrix}}^{\text{Fourier variables (in Fig. 3.28, from eqn (3.68))}}. \quad (3.69)$$

The trigonometric polynomial interpolating the points $\{x_0, \ldots, x_4\}$ is

$$x(\tau) = \underbrace{0.1104}_{c_1}\cdot\sin\left(\pi\frac{\tau}{\beta}\right) + \underbrace{0.2}_{c_2}\cdot\sin\left(2\pi\frac{\tau}{\beta}\right)\underbrace{-0.039}_{c_3}\cdot\sin\left(3\pi\frac{\tau}{\beta}\right), \quad (3.70)$$

and we easily check that $x(\frac{3}{4}\beta) = -0.15$, etc.

The weight of a path, a product of factors $\rho^{\text{free}}(x_k, x_{k+1}, \Delta_\tau)$, can be expressed through Fourier variables. To do so, we write out the weight as before, but without taking the $\Delta_\tau \to 0$ limit:

$$\left\{\begin{matrix}\text{weight}\\ \text{of path}\end{matrix}\right\} = \exp\left[-\mathcal{S}(\{x_0, \ldots, x_N\})\right]$$
$$= \exp\left[-\frac{(x_1 - x_0)^2}{2\Delta_\tau} - \frac{(x_2 - x_1)^2}{2\Delta_\tau} - \frac{(x_N - x_{N-1})^2}{2\Delta_\tau}\right]. \quad (3.71)$$

The action, $\mathcal{S}$, is transformed as

$$\sum_{k=1}^{N}\frac{(x_k - x_{k-1})^2}{2\Delta_\tau} = \frac{1}{2\Delta_\tau}\sum_{k=1}^{N}\sum_{n,l=1}^{N-1}c_n c_l$$
$$\times\left[\sin\left(n\pi\frac{k}{N}\right) - \sin\left(n\pi\frac{k-1}{N}\right)\right]\left[\sin\left(l\pi\frac{k}{N}\right) - \sin\left(l\pi\frac{k-1}{N}\right)\right].$$

Copyright © 2006. Oxford University Press, Incorporated. All rights reserved.

Krauth, Werner. Statistical Mechanics: Algorithms and Computations, Oxford University Press, Incorporated, 2006. ProQuest Ebook Central, http://ebookcentral.proquest.com/lib/tau/detail.action?docID=431021.
Created from tau on 2024-08-12 07:17:16.

Terms with $n \neq l$ vanish after summation over k, and we end up with:

$$\mathcal{S} = \frac{1}{2\Delta_\tau} \sum_{j=1}^{N-1} c_j^2 \sum_{k=1}^{N} \underbrace{\left[\sin\left(j\pi\frac{k}{N}\right) - \sin\left(j\pi\frac{k-1}{N}\right)\right]^2}_{4\cos^2\left[j\pi(k-\frac{1}{2})/N\right]\sin^2[j\pi/(2N)]}$$
$$= \frac{2}{\Delta_\tau} \sum_{n=1}^{N-1} c_n^2 \sin^2\left(\frac{n\pi}{2N}\right) \underbrace{\sum_{k=1}^{N} \cos^2\left[\frac{n\pi}{N}\left(k-\frac{1}{2}\right)\right]}_{N/2},$$

so that

$$\left\{\begin{array}{c}\text{weight}\\ \text{of path}\end{array}\right\} = \exp\left[-\frac{N}{\Delta_\tau}\sum_{n=1}^{N-1} c_n^2 \sin^2\left(\frac{n\pi}{2N}\right)\right]. \tag{3.72}$$

It is instructive to check that the weight of our example path from eqn (3.69) comes out the same no matter whether it is computed it from $\{x_0, \ldots, x_N\}$, using eqn (3.71), or from the $\{c_0, \ldots, c_N\}$, using eqn (3.72).

We have arrived at the representation of the path integral as

$$\rho^{\text{free}}(0,0,\beta) = \left\{\begin{array}{c}\text{sum of paths}\\ \text{from } 0 \to 0\end{array}\right\}$$
$$\propto \int_\infty^\infty \frac{\mathrm{d}c_1}{\sqrt{2\pi}\sigma_1} \ldots \frac{\mathrm{d}c_{N-1}}{\sqrt{2\pi}\sigma_{N-1}} \exp\left(-\frac{c_1^2}{2\sigma_1^2}\right) \ldots \exp\left(-\frac{c_{N-1}^2}{2\sigma_{N-1}^2}\right)$$
$$= \left[\int_\infty^\infty \frac{\mathrm{d}c_1}{\sqrt{2\pi}\sigma_1} \exp\left(-\frac{c_1^2}{2\sigma_1^2}\right)\right] \ldots \left[\int_\infty^\infty \frac{\mathrm{d}c_{N-1}}{\sqrt{2\pi}\sigma_{N-1}} \exp\left(-\frac{c_{N-1}^2}{2\sigma_{N-1}^2}\right)\right],$$

where

$$\sigma_n^2 = \frac{\beta}{2N^2 \sin^2\left(\frac{n\pi}{2N}\right)} \simeq \frac{2\beta}{\pi^2 n^2} + \cdots. \tag{3.73}$$

In the above representation of the path integral in Fourier space, the integrals are independent of each other. The Fourier modes are thus uncorrelated ($\langle c_k c_l \rangle \propto \delta_{kl}$), and the autocorrelations $\langle c_k c_k \rangle$, the variance of mode k, are given by eqn (3.73). This can be checked by generating paths with Alg. 3.5 (`levy-free-path`) and by Fourier-transforming them (see Fig. 3.29). Most simply, free paths are described as independent Gaussian modes n with zero mean and variance as $\propto 1/n^2$.

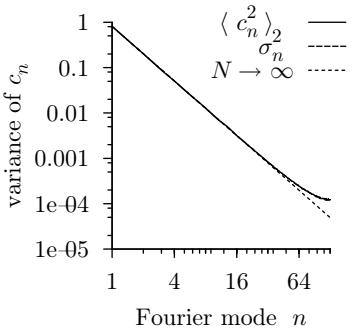

Fig. 3.29 Correlation $\langle c_n c_n \rangle$ of Fourier-transformed Lévy paths, compared to eqn (3.73) (from Alg. 3.5 (`levy-free-path`), with $N = 128$, $\beta = 4$).

Paths $\{x_0, \ldots, x_N\}$ can not only be described but also sampled as independent Gaussian Fourier modes, that is, as Gaussian random numbers $\{c_0, \ldots, c_N\}$ which can be transformed back to real space (see Alg. 3.12 (`fourier-free-path`)). This algorithm is statistically identical to the Lévy construction. Using fast Fourier methods, it can be implemented in $\propto N \log N$ operations.

In this subsection, we have passed back and forth between the real-space and the Fourier representation of paths, using classic formulas for expressing the $\{c_1, \ldots, c_N\}$ in terms of the $\{x_1, \ldots, x_N\}$ and vice versa. We saw how to transform the single path, but also the statistical weight

Copyright © 2006. Oxford University Press, Incorporated. All rights reserved.

Krauth, Werner. Statistical Mechanics: Algorithms and Computations, Oxford University Press, Incorporated, 2006. ProQuest Ebook Central, http://ebookcentral.proquest.com/lib/tau/detail.action?docID=431021.
Created from tau on 2024-08-12 07:17:16.

procedure `fourier-free-path`
for $n = 1, \ldots, N-1$ **do**
$\left\{ \begin{array}{l} \Upsilon_n \leftarrow 2N^2 \sin^2\left[n\pi/(2N)\right] \\ c_n \leftarrow \texttt{gauss}\left(\sqrt{\beta/\Upsilon_n}\right) \end{array} \right.$
for $k = 0, \ldots, N$ **do**
$\left\{ \begin{array}{l} x_k \leftarrow \sum_{n=1}^{N-1} c_n \sin\left(n\pi \frac{k}{N}\right) \end{array} \right.$
output $\{x_0, \ldots, x_N\}$

Algorithm 3.12 `fourier-free-path`. Sampling a path contributing to $\rho^{\rm free}(0,0,\beta)$ in Fourier space, and then transforming to real variables.

of a path, and the path integral itself. The path integral decoupled in Fourier space, because the real-space action is translation invariant.

We thus have two direct sampling algorithms: one in real space—the Lévy construction, and one in Fourier space—the independent sampling of modes. However, these algorithms exist for completely different reasons: the real-space algorithm relies on a local construction property of the sequence $\{x_1, \ldots, x_N\}$, which allows us to assemble pieces of the path independently of the other pieces. In contrast, the Fourier transformation decouples the real-space action because the latter is invariant under translations. In the case of the free path integral, Fourier transformation offered new insights, but did not really improve the performance of the Monte Carlo algorithms. In many other systems, however, simulations can be extremely difficult when done with one set of coordinates, and much easier after a coordinate transformations, because the variables might be less coupled. A simple example of such a system will be shown in Subsection 3.5.3, where a real-space Monte Carlo simulation would necessarily be very slow, but a Fourier-space calculation can proceed by direct sampling, that is, at maximum speed.

In this subsection we did not touch on the subject of fast Fourier transformation methods, which would allow us to pass between the $\{x_1, \ldots, x_N\}$ and the $\{c_1, \ldots, c_N\}$ in about $N \log N$ operations, rather than $\propto N^2$ (see for example Alg. 3.12 (`fourier-free-path`)). For heavy use of Fourier transformation, the fast algorithms must be implemented, using widely available routines. However, the naive versions provided by eqns (3.62) and (3.68) must always be kept handy, as alternative subroutines. They help us avoid problems with numerical factors of two and of π, and with subtle shifts of indices. As mentioned in many other places throughout this book, there is great virtue in getting to run naive algorithms before embarking on more elaborate, and less transparent programming endeavors.

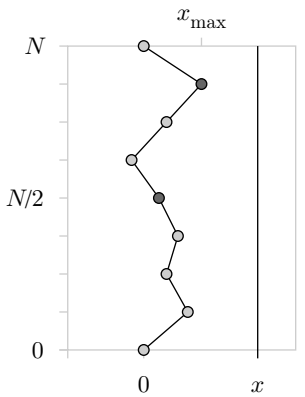

Fig. 3.30 Geometry of a path. We compute the probability distribution of the midpoint $x_{N/2}$, and the probability of staying to the left of x.

3.5.2 Path maxima, correlation functions

We continue to explore the geometry of free paths, which start and end at $x_0 = x_N = 0$. Let us compute first the probability distribution of the maximum of all x-values (see Fig. 3.30) i.e. the probability $\Pi_{\max}(x)$ for

Copyright © 2006. Oxford University Press, Incorporated. All rights reserved.

Krauth, Werner. Statistical Mechanics: Algorithms and Computations, Oxford University Press, Incorporated, 2006. ProQuest Ebook Central, http://ebookcentral.proquest.com/lib/tau/detail.action?docID=431021.
Created from tau on 2024-08-12 07:17:16.

the path to remain to the left of x. This path is contained in a box with the left wall at $-\infty$ and a right wall at x. It thus contributes to the density matrix $\rho^{\mathrm{box}[-\infty,\,x]}(0,0,\beta)$:

$$\rho^{\mathrm{box}[-\infty,\,x]}(0,0,\beta) = \lim_{L\to\infty} \rho^{\mathrm{box}[0,\,L]}(L-x,L-x,\beta)$$
$$\xrightarrow[\text{see eqn (3.23)}]{L\to\infty} \underbrace{\rho^{\mathrm{free}}(L-x,L-x,\beta)}_{\text{independent of } L \text{ and } x} - \underbrace{\rho^{\mathrm{free}}(L-x,L+x,\beta)}_{\text{from eqn (3.23)}},$$

because in an infinite box the sum over windings is dominated by a single flip operation. We find

$$\Pi_{\max}(x) = \left\{ \begin{array}{c} \text{prob. that} \\ \text{max. position} < x \end{array} \right\} = \frac{\rho^{\mathrm{box}[-\infty,\,x]}(0,0,\beta)}{\rho^{\mathrm{free}}(0,0,\beta)}$$
$$= \frac{\rho^{\mathrm{free}}(x,x,\beta) - \rho^{\mathrm{free}}(-x,x,\beta)}{\rho^{\mathrm{free}}(x,x,\beta)} = 1 - \exp\left(-\frac{2x^2}{\beta}\right).$$

The probability $\Pi_{\max}(x+\mathrm{d}x)$ counts all paths whose maximum is to the left of $x+\mathrm{d}x$, and $\Pi_{\max}(x)$ counts all those paths whose maximum position is smaller than x. The difference between the two amounts to all paths whose maximum falls between x and $x+\mathrm{d}x$. Therefore,

$$\pi_{\max}(x) = \left\{ \begin{array}{c} \text{prob. that} \\ x_{\max} = x \end{array} \right\} = \frac{\mathrm{d}\Pi_{\max}(x)}{\mathrm{d}x} = \frac{4x}{\beta} \exp\left(-\frac{2x^2}{\beta}\right) \qquad (3.74)$$

(see Fig. 3.31).

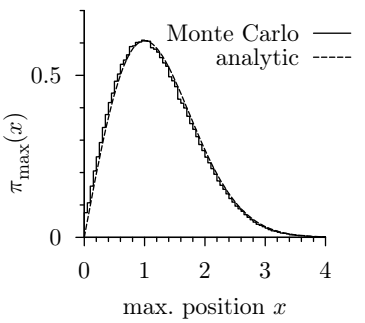

Fig. 3.31 Distribution of the path maximum (with $\beta = 4$, from modified Alg. 3.5 (`levy-free-path`), compared with eqn (3.74)).

After the maximum positions, we now consider correlations $\langle x_k x_l \rangle$ between the different components of a path $\{x_0, \ldots, x_N\}$. The autocorrelation of $x_{N/2}$ (see Fig. 3.30) follows, for $N \to \infty$, from the Fourier representation (3.60) of $x_{N/2}$:

$$\left\langle x_{\frac{N}{2}} x_{\frac{N}{2}} \right\rangle = \sum_{k=1}^{\infty} \sigma_k^2 \underbrace{\sin^2 \frac{\pi k}{2}}_{\substack{0 \text{ for } k=2,4,\ldots \\ 1 \text{ for } k=1,3,\ldots}} \to \frac{2\beta}{\pi^2} \underbrace{\left(1 + \frac{1}{3^2} + \frac{1}{5^2} + \cdots\right)}_{\pi^2/8} = \frac{\beta}{4}. \quad (3.75)$$

This correlation is in fact independent of N, as we can see as follows. The probability distribution of the midpoint (corresponding to slice $N/2$ or, equivalently, to imaginary time $\tau = \beta/2$) is

$$\pi_{\beta/2}(x) = \frac{\rho^{\mathrm{free}}(0,x,\frac{\beta}{2})\,\rho^{\mathrm{free}}(x,0,\frac{\beta}{2})}{\rho^{\mathrm{free}}(0,0,\beta)} = \sqrt{\frac{2}{\pi\beta}} \exp\left(-\frac{2x^2}{\beta}\right),$$

a Gaussian with zero mean and variance $\sigma^2 = \langle x^2 \rangle = \beta/4$ $\langle x^2 \rangle = \beta/4$, in agreement with eqn (3.75). The root mean square width of the path grows with the square root of the length β of the path, that is, with $\sqrt{\beta}$. This relation, (width) $\propto \sqrt{(\text{length})}$, is the hallmark of diffusive processes, and of random walks.

We now determine all the path correlations $\langle x_k x_l \rangle$ from the path integral action. Using for concreteness $\Delta_\tau = 1$ so that $N = \beta$, the action is

$$\mathcal{S} = \frac{1}{2}\left[(x_1 - x_0)^2 + \cdots + (x_N - x_{N-1})^2\right].$$

Copyright © 2006. Oxford University Press, Incorporated. All rights reserved.

Krauth, Werner. Statistical Mechanics: Algorithms and Computations, Oxford University Press, Incorporated, 2006. ProQuest Ebook Central, http://ebookcentral.proquest.com/lib/tau/detail.action?docID=431021.
Created from tau on 2024-08-12 07:17:16.

With $x_0 = x_N = 0$, the action $\mathcal{S}$ can be written in matrix form:

$$\left\{ \begin{matrix} \text{weight of} \\ \text{path} \end{matrix} \right\} \propto \exp\left(-\frac{1}{2} \sum_{k,l=1}^{N-1} x_k \mathcal{M}_{kl} x_l \right).$$

Let us look at this $(N-1)\times(N-1)$ matrix, and its inverse, for $N = 8$:

$$\underbrace{\begin{bmatrix} 2 & -1 & \cdot & \cdot & \cdot & \cdot & \cdot \\ -1 & 2 & -1 & \cdot & \cdot & \cdot & \cdot \\ \cdot & -1 & 2 & -1 & \cdot & \cdot & \cdot \\ \cdot & \cdot & -1 & 2 & -1 & \cdot & \cdot \\ \cdot & \cdot & \cdot & -1 & 2 & -1 & \cdot \\ \cdot & \cdot & \cdot & \cdot & -1 & 2 & -1 \\ \cdot & \cdot & \cdot & \cdot & \cdot & -1 & 2 \end{bmatrix}^{-1}}_{\mathcal{M} \text{ (in action } \mathcal{S})} = \frac{1}{8} \underbrace{\begin{bmatrix} 7 & 6 & 5 & 4 & 3 & 2 & 1 \\ 6 & 12 & 10 & 8 & 6 & 4 & 2 \\ 5 & 10 & 15 & 12 & 9 & 6 & 3 \\ 4 & 8 & 12 & 16 & 12 & 8 & 4 \\ 3 & 6 & 9 & 12 & 15 & 10 & 5 \\ 2 & 4 & 6 & 8 & 10 & 12 & 6 \\ 1 & 2 & 3 & 4 & 5 & 6 & 7 \end{bmatrix}}_{\mathcal{M}^{-1} \text{ (correlation matrix } (\langle x_k x_l \rangle))}, \quad (3.76)$$

as is easily checked. In general, the inverse of the $(N-1)\times(N-1)$ matrix $\mathcal{M}$ of eqn (3.76) is

$$\mathcal{M}^{-1}_{kl} = \frac{1}{N} \min\left[(N-k)l, (N-l)k\right].$$

For the free path integral, the correlation functions are given by the inverse of the matrix $\mathcal{M}$:

$$\langle x_k x_l \rangle = (\mathcal{M}^{-1})_{kl} = \frac{\int \mathrm{d}x_1 \ldots \mathrm{d}x_{N-1} x_k x_l \exp\left(-\frac{1}{2}\sum x_n \mathcal{M}_{nm} x_m\right)}{\int \mathrm{d}x_1 \ldots \mathrm{d}x_{N-1} \exp\left(-\frac{1}{2}\sum x_n \mathcal{M}_{nm} x_m\right)}. \quad (3.77)$$

The general correlation formula in eqn (3.77) agrees with the mid-path correlation (eqn (3.75)), because

$$(\mathcal{M}^{-1})_{44} = \frac{16}{8} = \frac{\beta}{4}$$

(we note that in eqn (3.76), we supposed $\beta = N = 8$). Equation (3.77) has many applications. We use it here to prove the correctness of a trivial sampling algorithm for free paths, which generates a first path $\{\Upsilon_0, \ldots, \Upsilon_N\}$ from a sum of uncorrelated Gaussian random numbers, without taking into account that the path should eventually return to $x = 0$. We define

$$\Upsilon_k = \begin{cases} 0 & \text{for } k = 0 \\ \Upsilon_{k-1} + \xi_k & \text{for } k = 1, \ldots, N \end{cases},$$

where ξ_k are uncorrelated Gaussian random numbers with variance 1. After the construction of this first path, we "pull back" Υ_N to zero (by an amount Υ_N). For all k, Υ_k is pulled back by $\Upsilon_N k/N$ (see Alg. 3.13 (`trivial-free-path`) and Fig. 3.32). The pulled-back random variables η_k (which are correlated) are also sums of the uncorrelated Gaussians ξ_k, and their variances depend on k:

$$\eta_k = \underbrace{\xi_1 + \cdots + \xi_k}_{\Upsilon_k} - \frac{k}{N}\underbrace{(\xi_1 + \cdots + \xi_N)}_{\Upsilon_N} = \sum_{l=1}^{N} a_{kl} \xi_l,$$

Copyright © 2006. Oxford University Press, Incorporated. All rights reserved.

Krauth, Werner. Statistical Mechanics: Algorithms and Computations, Oxford University Press, Incorporated, 2006. ProQuest Ebook Central, http://ebookcentral.proquest.com/lib/tau/detail.action?docID=431021.
Created from tau on 2024-08-12 07:17:16.

where

$$a_{kl} = \begin{cases} 1 - \frac{k}{N} & \text{if } l \le k \\ -\frac{k}{N} & \text{if } l > k \end{cases}.$$

procedure `trivial-free-path`
$x_0 \leftarrow 0, \Upsilon_0 \leftarrow 0$
for $k = 1, \ldots, N$ **do**
  $\{\ \Upsilon_k \leftarrow \Upsilon_{k-1} + \texttt{gauss}\,(\sqrt{\beta/N})$
for $k = 1, \ldots, N$ **do**
  $\{\ x_k \leftarrow \Upsilon_k - \Upsilon_N k/N$
output $\{x_0, \ldots, x_N\}$

Algorithm 3.13 `trivial-free-path`. Sampling a path contributing to $\rho^{\text{free}}(0, 0, \beta)$ with a trivial, yet correct, algorithm (see Fig. 3.32).

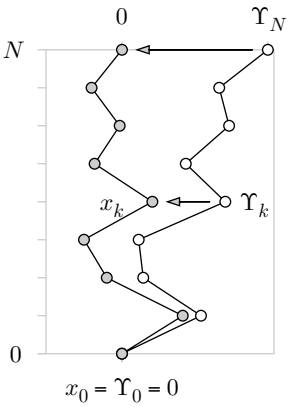

Fig. 3.32 Direct sampling of a path contributing to $\rho^{\text{free}}(0, 0, \beta)$ by pulling back an unrestricted path.

The Gaussians η_k are characterized by their means, which are all zero, and by their correlations which, for $k \le l$, are given by

$$\langle \eta_k \eta_l \rangle = \frac{\beta}{N} \sum_{j=1}^{N} a_{kj} a_{lj}$$
$$= \frac{1}{N^2} [\underbrace{k(N-k)(N-l)}_{j \le k} - \underbrace{(l-k)k(N-l)}_{k < j \le l} + \underbrace{(N-l)kl}_{l \le j}] = \underbrace{\frac{1}{N} k(N-l)}_{\text{see eqn (3.77)}}.$$

This agrees with the correlation matrix of the path integral. We see that the random variables $\{\eta_0, \ldots, \eta_N\}$ from Alg. 3.13 (`trivial-free-path`) indeed sample paths contributing to the free density matrix.

3.5.3 Classical random paths

In this chapter, we have discussed a number of direct path-sampling algorithms for the free density matrix. All these algorithms produced statistically identical output, both for discrete paths and in the continuum limit. Performances were also roughly equivalent. What really differentiates these algorithms is how they generalize from the free paths (classical random walks). We saw, for example, that the Lévy construction can be made to sample harmonic-oscillator paths (see Subsection 3.3.2).

In the present subsection, we consider generalized Fourier sampling methods. For concreteness, we restrict our attention to the continuous paths with $\Delta_\tau = \beta/N \to 0$. In Fourier space, continuous paths are generated by independent Gaussian random variables with variance $\propto 1/n^2$, for all $n = \{1, 2, \ldots\}$ (see Alg. 3.12 (`fourier-free-path`)). We now analyze the paths that arise from a scaling $\propto 1/n^\alpha$ of the variances. We again pass between the real-space and the Fourier representations, and adopt the most general Fourier transform, containing sines and cosines:

$$x(t) = \sum_{n=1}^{\infty} \left\{ a_n \cos\left(2n\pi \frac{t}{L}\right) + b_n \sin\left(2n\pi \frac{t}{L}\right) \right\}. \tag{3.78}$$

Copyright © 2006. Oxford University Press, Incorporated. All rights reserved.

Krauth, Werner. Statistical Mechanics: Algorithms and Computations, Oxford University Press, Incorporated, 2006. ProQuest Ebook Central, http://ebookcentral.proquest.com/lib/tau/detail.action?docID=431021.
Created from tau on 2024-08-12 07:17:16.

The paths described by eqn (3.78) have zero mean ($\int_0^L \mathrm{d}t\; x(t)/L = 0$), but need not start at the origin $x = 0$. The Fourier-space action in eqn (3.64) can be written for the transform in eqn (3.78) and generalized to arbitrary values of α:

$$\mathcal{S} = \frac{1}{2}\sum_{n=1}^{\infty}\left(\frac{2\pi n}{L}\right)^{\alpha}\int_0^L \mathrm{d}t\;\left[a_n^2\cos^2\left(2n\pi\frac{t}{L}\right) + b_n^2\sin^2\left(2n\pi\frac{t}{L}\right)\right]$$
$$= \frac{1}{2}\sum_n \underbrace{\left(\frac{2\pi n}{L}\right)^{\alpha}\frac{L}{2}}_{\sigma_n^{-2}}(a_n^2 + b_n^2). \quad (3.79)$$

The a_n and b_n are Gaussian random variables with standard deviation

$$\sigma_n = \frac{1}{(\pi n)^{1/2}}\left(\frac{L}{2\pi n}\right)^{\alpha/2-\frac{1}{2}}. \quad (3.80)$$

The roughness exponent $\zeta = \alpha/2 - \frac{1}{2}$ in eqn (3.80) gives the scaling of the root mean square width of the path to its length so that we now have (width) $\propto$ (length)$^{\zeta}$ (ζ is pronounced "zeta"). All quantum paths, and all random walks have $\zeta = \frac{1}{2}$. However, many other paths appearing in nature are characterized by roughness exponents ζ different from $\frac{1}{2}$. Predicting these exponents for a given physical phenomenon is beyond the scope of this book. In this subsection, our goal is more restricted. We only aim at characterizing Gaussian paths, the simplest paths with nontrivial roughness exponents (with $0 < \zeta < 1$), and which are governed by the action in eqn (3.79).

procedure `fourier-gen-path`
for $n = 1, 2, \ldots$ **do**
$\left\{\begin{array}{l} \sigma_n \leftarrow (\pi n)^{-\frac{1}{2}}\left(\frac{L}{2\pi n}\right)^{\zeta} \\ a_n \leftarrow \texttt{gauss}\,(\sigma_n) \\ b_n \leftarrow \texttt{gauss}\,(\sigma_n) \end{array}\right.$
for $t = 0, \Delta_t, \ldots, L$ **do**
$\left\{\; x(t) \leftarrow \sum_{n=1}^{\infty}\left[a_n\cos\left(2n\pi\frac{t}{L}\right) + b_n\sin\left(2n\pi\frac{t}{L}\right)\right]\right.$
output $\{x(0), \ldots, x(L)\}$

Algorithm 3.14 `fourier-gen-path`. Sampling a periodic Gaussian path with roughness ζ.

Periodic Gaussian paths can be easily sampled for various roughness exponents (see Fig. 3.33 and Alg. 3.14 (`fourier-gen-path`)). As discussed, the paths with larger ζ grow faster on large scales, but we see that they are also smoother, because the Fourier coefficients vanish faster as $n \to \infty$. Some paths appear wider than others (see Fig. 3.33). This is not a finite-size effect, as we can see as follows. A larger interval L is generated by rescaling $L \to \Upsilon L$. Under this rescaling, the standard deviations of the Gaussian random numbers in Alg. 3.14 (`fourier-gen-path`) are

Copyright © 2006. Oxford University Press, Incorporated. All rights reserved.

Krauth, Werner. Statistical Mechanics: Algorithms and Computations, Oxford University Press, Incorporated, 2006. ProQuest Ebook Central, http://ebookcentral.proquest.com/lib/tau/detail.action?docID=431021.
Created from tau on 2024-08-12 07:17:16.

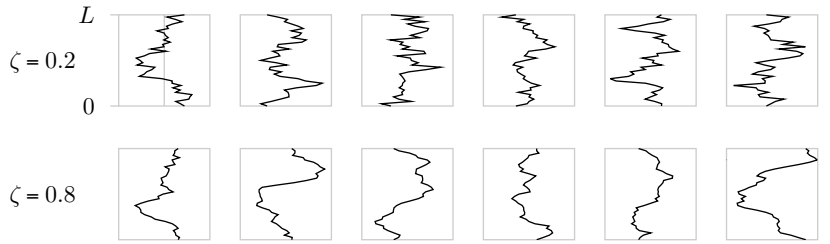

Fig. 3.33 Periodic Gaussian paths with two different roughness exponents (from Alg. 3.14 (`fourier-gen-path`), with 40 Fourier modes).

uniformly rescaled as $\sigma_n \to \Upsilon^\zeta \sigma_n$. Under this transformation, each individual path is rescaled by factors Υ in t (length) and Υ^ζ in x (width), but its shape remains unchanged. The same rescaling applies also to the ensemble of all paths; they are self-affine.

We can define the (mean square) width of a path as follows:

$$\omega_2 = \frac{1}{L}\int_0^L \mathrm{d}x\; x^2(t)$$

(we remember that the average position is zero). Wide paths have a larger value of ω_2 than narrow paths. We can compute the probability distribution of the width, $\pi_\zeta(\omega_2)$, using Alg. 3.14 (`fourier-gen-path`) (see Fig. 3.36, later).

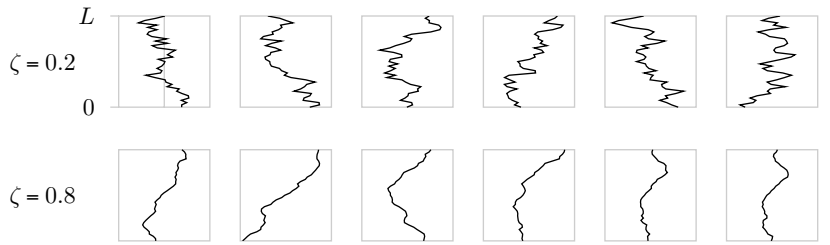

Fig. 3.34 Free Gaussian paths with two different roughness exponents (from Alg. 3.15 (`fourier-cos-path`), with 40 Fourier modes).

However, Alg. 3.14 (`fourier-gen-path`) is not a unique prescription for generating Gaussian paths with roughness exponent ζ. We can also generalize the Fourier sine transform of Subsection 3.5.1, or generate the paths by a Fourier cosine series:

$$x(t) = \sum_{n=1}^{\infty} c_n \cos\left(n\pi\frac{t}{L}\right),$$

Copyright © 2006. Oxford University Press, Incorporated. All rights reserved.

Krauth, Werner. Statistical Mechanics: Algorithms and Computations, Oxford University Press, Incorporated, 2006. ProQuest Ebook Central, http://ebookcentral.proquest.com/lib/tau/detail.action?docID=431021.
Created from tau on 2024-08-12 07:17:16.

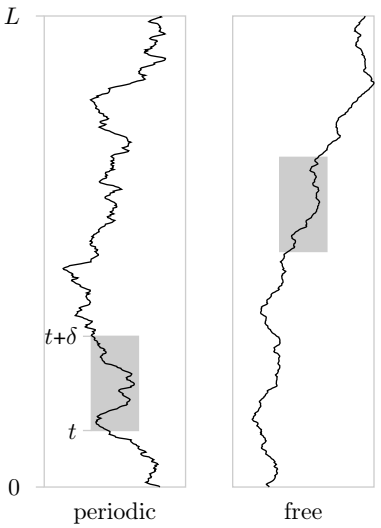

Fig. 3.35 Periodic and free Gaussian paths with $\zeta = 0.8$. In small intervals $[t, t+\delta]$, with $\delta/L \to 0$, path fragments are statistically identical.

where the c_n are again independent Gaussian random variables with a ζ-dependent scaling (see Alg. 3.15 (`fourier-cos-path`) and Fig. 3.34). In these "free" paths, the boundary conditions no longer identify $x(0)$ and $x(L)$.

procedure `fourier-cos-path`
for $n = 1, 2, \ldots$ **do**
$\left\{ \begin{array}{l} \sigma_n \leftarrow \frac{2}{\pi n} \left(\frac{L}{\pi n}\right)^{\zeta} \\ c_n \leftarrow \texttt{gauss}\,(\sigma_n) \end{array} \right.$
for $t = 0, \Delta_t, \ldots, L$ **do**
$\left\{ \; x(t) \leftarrow \sum_{n=1}^{\infty} c_n \cos\left(n\pi \frac{t}{L}\right) \right.$
output $\{x(0), \ldots, x(L)\}$

Algorithm 3.15 `fourier-cos-path`. Sampling a free Gaussian path with roughness exponent ζ.

The periodic paths in Fig. 3.33 differ from the free paths in Fig. 3.34 not only in the boundary conditions, but also in the width distributions. Nevertheless, the statistical properties of path fragments are equivalent in a small interval $[t, t+\delta]$, with $\delta/L \to 0$, for $\delta \ll t \ll L$ (see Fig. 3.35). To show this, we consider the mean value of the path fragment,

$$\langle x \rangle_{t,\delta} = \frac{1}{\delta} \int_t^{t+\delta} \mathrm{d}t \; x(t'),$$

and the width of a path fragment,

$$\omega_2(t, \delta) = \int_t^{t+\delta} \mathrm{d}t' \; \left[x(t') - \langle x \rangle_{t,\delta} \right]^2 .$$

We rescale the distribution of ω_2 such that its mean value is equal to 1. To obtain the width of a path fragment, we either generate the whole path from the explicit routines of this subsection or compute the width directly from the Fourier decomposition without generating $x(t)$. This is possible because a path fragment which is defined by Fourier coefficients $\{c_1, c_2, \ldots\}$ has width

$$\omega_2(t, \delta) = \sum_{n,m=1}^{\infty} c_n c_m D_{nm}(t, \delta), \tag{3.81}$$

where the coefficients $D_{nm}(t, \delta)$ are given by

$$D_{nm}(t, \delta) = \frac{1}{\delta} \int_t^{t+\delta} \mathrm{d}t' \overbrace{\cos\left(n\pi t'\right) \cos\left(m\pi t'\right)}^{\frac{1}{2}\left\{\cos\left[(m-n)\pi t'\right] + \cos\left[(m+n)\pi t'\right]\right\}} - \frac{1}{\delta^2} \left[\int_t^{t+\delta} \mathrm{d}t' \; \cos\left(n\pi t'\right) \right] \left[\int_t^{t+\delta} \mathrm{d}t' \; \cos\left(m\pi t'\right) \right].$$

Copyright © 2006. Oxford University Press, Incorporated. All rights reserved.

Krauth, Werner. Statistical Mechanics: Algorithms and Computations, Oxford University Press, Incorporated, 2006. ProQuest Ebook Central, http://ebookcentral.proquest.com/lib/tau/detail.action?docID=431021.
Created from tau on 2024-08-12 07:17:16.

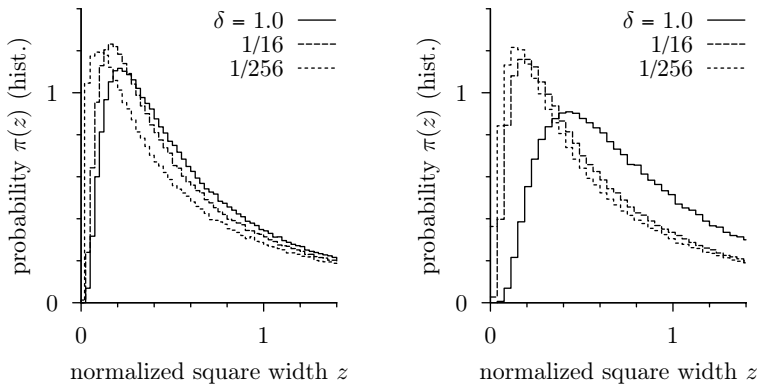

Fig. 3.36 Width fluctuations (normalized) for free paths (*left*) and for periodic paths (*right*) with $\zeta = 0.75$ (from eqn (3.81), with $z = \omega_2 / \langle \omega_2 \rangle$).

These integrals can be computed analytically, once and for all. The width $\omega_2(t, \delta)$ of each path is then obtained directly from eqn (3.81), with coefficients c_n taken from Alg. 3.15 (`fourier-cos-path`). The distribution of $\omega_2(t, \delta)$ can then be determined as an average over many paths. One can redo an analogous calculation for periodic paths (one finds three sets of coefficients, one for the sine–sine integrals, one for cosine–cosine integrals, and one for the mixed terms). For $\delta = 1$, the width distributions are quite different, but they converge to the same curve in the limit $\delta / L \to 0$ (see Fig. 3.36). For free paths, the width distribution depends on the length of the interval δ and also on the starting point gt (for $\zeta \neq \frac{1}{2}$). For periodic paths, the distribution is independent of t because of translational invariance.

In conclusion, this subsection introduced Gaussian paths, which allow us to describe real paths in nature, from the notorious random walk (with $\alpha = 2$, $\zeta = \frac{1}{2}$), to cracks, interfaces, and phase boundaries, among many others. A rough numerical simulation allowed us to show that the statistical properties of small path fragments become independent of the boundary condition. This statement can be made mathematically rigorous (see Rosso, Santachiara, and Krauth (2005)).

Copyright © 2006. Oxford University Press, Incorporated. All rights reserved.

Krauth, Werner. Statistical Mechanics: Algorithms and Computations, Oxford University Press, Incorporated, 2006. ProQuest Ebook Central, http://ebookcentral.proquest.com/lib/tau/detail.action?docID=431021.
Created from tau on 2024-08-12 07:17:16.

Exercises

(Section 3.1)

(3.1) Use Alg. 3.1 (`harmonic-wavefunction`) to generate the wave functions $\{\psi_0^{\text{h.o.}}(x), \ldots, \psi_{20}^{\text{h.o.}}(x)\}$ on a fine grid in the interval $x \in [-5, 5]$. Verify numerically that the wave functions are normalized and mutually orthogonal, and that they solve the Schrödinger equation (eqn (3.1)) with $\hbar = m = \omega = 1$. Analytically prove that the normalization is correct and that the wave functions are mutually orthogonal. Use the recursion relation to show analytically that the wave functions solve the Schrödinger equation.
NB: For the numerical checks, note that, on a grid with step size Δ_x, the gradient is

$$\frac{\partial}{\partial x}\psi(x_k) \simeq \frac{\psi(x_{k+1}) - \psi(x_k)}{\Delta_x},$$

and the second derivative is approximated as

$$\begin{aligned}\frac{\partial^2}{\partial x^2}\psi(x_k) &\simeq \frac{1}{\Delta_x}\left[\frac{\partial}{\partial x}\psi(x_k) - \frac{\partial}{\partial x}\psi(x_{k-1})\right] \\ &\simeq \frac{\psi(x_{k+1}) - 2\psi(x_k) + \psi(x_{k-1})}{\Delta_x^2}.\end{aligned}$$

(3.2) Determine the density matrix of the harmonic oscillator using Algs 3.2 (`harmonic-density`) and 3.1 (`harmonic-wavefunction`). Plot the diagonal density matrix $\rho^{\text{h.o.}}(x, x, \beta)$ for several temperatures. What is its relationship between the density matrix and the probability $\pi(x)$ of the quantum particle to be at position x? Compare this probability with the Boltzmann distribution $\pi(x)$ for a classical particle of mass $m = 1$ in a potential $V(x) = \frac{1}{2}x^2$.

(3.3) Familiarize yourself with the calculation, in eqn (3.10), of the free density matrix using plane-wave functions in an infinite box with periodic boundary conditions (pay attention to the use of the dummy parameter Δ_n). Alternatively determine the free density matrix using the wave functions (eqn (3.20)) in a box with hard walls at positions $x = -L/2$ and $x = L/2$ in the limit $L \to \infty$.
NB: First shift the functions in eqn (3.20) by $L/2$ to the left.
Finally, to illustrate the calculation of density matrices in arbitrary bases, expand the free density matrix in the harmonic oscillator basis:

$$\langle\psi_n^{\text{h.o.}}|H^{\text{free}}|\psi_m^{\text{h.o.}}\rangle = \langle\psi_n^{\text{h.o.}}|H^{\text{h.o.}} - \frac{1}{2}x^2|\psi_m^{\text{h.o.}}\rangle.$$

Derive an explicit formula for $\langle\psi_n^{\text{h.o.}}|x^2|\psi_m^{\text{h.o.}}\rangle$ from the recursion relation used in Alg. 3.1 (`harmonic-wavefunction`). Use the results of these calculations to compute numerically the density matrix as $\rho_{nm} = 1 - \beta H_{nm} + \frac{\beta^2}{2}\left(H^2\right)_{nm} - \cdots +$ and also

$$\rho^{\text{free}}(x, x', \beta) = \sum_{n,m=0}^{\infty} \psi_n^{\text{h.o.}}(x)\rho_{nm}\psi_m^{\text{h.o.}}(x').$$

Compare the density matrix obtained with the exact solution.

(Section 3.2)

(3.4) Implement Alg. 3.3 (`matrix-square`) on a fine grid of equidistant points. Start from the high-temperature density matrix in eqn (3.30), and iterate several times, doubling β at each time. Compare your results with the exact density matrix for the harmonic oscillator (eqn (3.37)).

(3.5) Consider the exactly solvable Pöschl–Teller potential

$$V(x) = \frac{1}{2}\left[\frac{\chi(\chi-1)}{\sin^2 x}\frac{\lambda(\lambda-1)}{\cos^2 x}\right].$$

Plot this potential for several choices of $\chi > 1$ and $\lambda > 1$, with x in the interval $[0, \pi/2]$. The energy eigenvalues of a particle of mass $m = 1$ in this potential are

$$E_n^{\text{P–T}} = \frac{1}{2}(\chi + \lambda + 2n)^2 \quad \text{for } n = 0, \ldots, \infty.$$

All the wave functions are known analytically, and the ground state has the simple form:

$$\psi_0^{\text{P–T}}(x) = \text{const} \cdot \sin^{\chi} x \ \cos^{\lambda} x \quad x \in [0, \pi/2].$$

Use the Trotter formula, and matrix squaring (Alg. 3.3 (`matrix-square`)), to compute the density matrix $\rho^{\text{P–T}}(x, x', \beta)$ at arbitrary temperature. Plot its diagonal part at low temperatures, and show that

$$\rho^{\text{P–T}}(x, x, \beta) \xrightarrow[\beta\to\infty]{} \text{const} \cdot \left[\psi_0^{\text{P–T}}(x)\right]^2,$$

for various values of χ and λ. Can you deduce the value of $E_0^{\text{P–T}}$ from the output of the matrix-squaring routine? Compute the partition function

Copyright © 2006. Oxford University Press, Incorporated. All rights reserved.

Krauth, Werner. Statistical Mechanics: Algorithms and Computations, Oxford University Press, Incorporated, 2006. ProQuest Ebook Central, http://ebookcentral.proquest.com/lib/tau/detail.action?docID=431021.
Created from tau on 2024-08-12 07:17:16.

$Z^{\mathrm{P-T}}(\beta)$ using matrix squaring, and compare with the explicit solution given by the sum over eigenvalues $E_n^{\mathrm{P-T}}$. Check analytically that $\psi_0^{\mathrm{P-T}}(x)$ is indeed the ground-state wave function of the Pöschl–Teller potential.

(3.6) In Section 3.2.1, we derived the second-order Trotter formula for the density matrix at high temperature. Show that the expression

$$\rho\left(x, x', \Delta_\tau\right) \simeq \rho^{\mathrm{free}}\left(x, x', \Delta_\tau\right) \mathrm{e}^{-\Delta_\tau V(x')}$$

is correct only to first order in Δ_τ. Study the becomings of this first-order approximation under the convolution in eqn (3.32), separately for diagonal matrix elements $\rho(x, x, \Delta_\tau)$ and for nondiagonal elements $\rho(x, x', \Delta_\tau)$, each at low temperature (large $\beta = N\Delta_\tau$).

(3.7) Consider a particle of mass $m = 1$ in a box of size L. Compute the probability $\pi^{\mathrm{box}}(x)$ to be at a position x, and inverse temperature β, in three different ways: first, sum explicitly over all states (adapt Alg. 3.2 (`harmonic-density`) to the box wave functions of eqn (3.20), with eigenvalues $E_n = \frac{1}{2}(n\pi/L)^2$). Second, use Alg. 3.3 (`matrix-square`) to compute $\rho^{\mathrm{box}}(x, x', \beta)$ from the high-temperature limit

$$\rho^{\mathrm{box}}\left(x, x', \beta\right) = \begin{cases} \rho^{\mathrm{free}}(x, x', \beta) & \text{if } 0 < x, x' < L \\ 0 & \text{otherwise} \end{cases}.$$

Finally, compute $\pi^{\mathrm{box},L}(x)$ from the density-matrix expression in eqn (3.23). Pay attention to the different normalizations of the density matrix and the probability $\pi^{\mathrm{box}}(x)$.

(Section 3.3)

(3.8) Implement Alg. 3.4 (`naive-harmonic-path`). Check your program by plotting a histogram of the positions x_k for $k = 0$ and for $k = N/2$. Verify that the distributions $\pi(x_0)$ and of $\pi(x_{N/2})$ agree with each other and with the analytic form of $\rho^{\mathrm{h.o.}}(x, x, \beta)/Z$ (see eqn (3.38)).

(3.9) Implement the Lévy construction for paths contributing to the free density matrix (Alg. 3.5 (`levy-free-path`)). Use this subroutine in an improved path-integral simulation of the harmonic oscillator (see Exerc. 3.8): cut out a connected piece of the path, between time slices k and k' (possible across the horizon), and thread in a new piece, generated with Alg. 3.5 (`levy-free-path`). Determine the acceptance probabilities in the Metropolis algorithm, taking into account that the free-particle Hamiltonian is already incorporated in the Lévy-construction. Run your program for a sufficiently long time to allow careful comparison with the exact solution (see eqn (3.38)).

(3.10) Use Markov-chain methods to sample paths contributing to the partition function of a particle in the Pöschl–Teller potential of Exerc. 3.5. As in Exerc. 3.9, cut out a piece of the path, between time slices k and k' (possibly across the horizon), and thread in a new path, again generated with Alg. 3.5 (`levy-free-path`) (compare with Exerc. 3.9). Correct for effects of the potential using the Metropolis algorithm, again taking into account that the free Hamiltonian is already incorporated in the Lévy construction. If possible, check Monte Carlo output against the density matrix $\rho^{\mathrm{P-T}}(x, x, \beta)$ obtained in Exerc. 3.5. Otherwise, check consistency at low temperature with the ground-state wave function $\psi_0^{\mathrm{P-T}}(x)$ quoted in Exerc. 3.5.

(3.11) Use Alg. 3.8 (`naive-box-path`) in order to sample paths contributing to $\rho^{\mathrm{box}}(x, x', \beta)$. Generalize to sample paths contributing to $Z^{\mathrm{box}}(\beta)$ (sample $x_0 = x_N$ from the diagonal density matrix, as in Fig. 3.15, then use Alg. 3.8 (`naive-box-path`)). Sketch how this naive algorithm can be made into a rejection-free direct sampling algorithm, using the exact solution for $\rho^{\mathrm{box}}(x, x', \beta)$ from eqn (3.47). Implement this algorithm, using a fine grid of x-values in the interval $[0, L]$.
NB: In the last part, use tower sampling, from Alg. 1.14 (`tower-sample`), to generate x-values.

(Section 3.5)

(3.12) Compare the three direct-sampling algorithms for paths contributing to $\rho^{\mathrm{free}}(0, 0, \beta)$, namely Alg. 3.5 (`levy-free-path`), Alg. 3.12 (`fourier-free-path`), and finally Alg. 3.13 (`trivial-free-path`). Implement them. To show that they lead to equivalent results, Compute the correlation functions $\langle x_k x_l \rangle$. Can each of these algorithms be generalized to sample paths contributing to $\rho^{\mathrm{h.o.}}(0, 0, \beta)$?

(3.13) Generate periodic random paths with various roughness exponents $0 < \zeta < 1.5$ using Alg. 3.14 (`fourier-gen-path`). Plot the mean square width ω_2 as a function of L. For given L, determine the scaling of the mean square deviation $\left\langle |x(t) - x(0)|^2 \right\rangle$ as a function of t. Explain why these two quantities differ qualitatively for $\zeta > 1$ (see Leschhorn and Tang (1993)).

Copyright © 2006. Oxford University Press, Incorporated. All rights reserved.

Krauth, Werner. Statistical Mechanics: Algorithms and Computations, Oxford University Press, Incorporated, 2006. ProQuest Ebook Central, http://ebookcentral.proquest.com/lib/tau/detail.action?docID=431021.
Created from tau on 2024-08-12 07:17:16.

References

Feynman R. P. (1972) *Statistical Mechanics: A Set of Lectures*, Benjamin/Cummings, Reading, Massachusetts

Hess G. B., Fairbank W. M. (1967) Measurement of angular momentum in superfluid helium, *Physical Review Letters* **19**, 216–218

Krauth W. (1996) Quantum Monte Carlo calculations for a large number of bosons in a harmonic trap, *Physical Review Letters* **77**, 3695–3699

Leggett A. J. (1973) Topics in the theory of helium, *Physica Fennica* **8**, 125–170

Leschhorn H., Tang L. H. (1993) Elastic string in a random potential–comment, *Physical Review Letters* **70**, 2973

Lévy P., (1940) Sur certains processus stochastiques homogènes [in French], *Composition Mathematica* **7**, 283–339

Pollock E. L., Ceperley D. M. (1984) Simulation of quantum many-body systems by path-integral methods, *Physical Review B* **30**, 2555–2568

Pollock E. L., Ceperley D. M. (1987) Path-integral computation of superfluid densities, *Physical Review B* **36**, 8343–8352

Rosso A., Santachiara R., Krauth W. (2005) Geometry of Gaussian signals, *Journal of Statistical Mechanics: Theory and Experiment*, L08001

Storer R. G. (1968) Path-integral calculation of quantum-statistical density matrix for attractive Coulomb forces, *Journal of Mathematical Physics* **9**, 964–970

Copyright © 2006. Oxford University Press, Incorporated. All rights reserved.

Krauth, Werner. Statistical Mechanics: Algorithms and Computations, Oxford University Press, Incorporated, 2006. ProQuest Ebook Central, http://ebookcentral.proquest.com/lib/tau/detail.action?docID=431021.
Created from tau on 2024-08-12 07:17:16.